BIOMEDICAL SIGNAL ANALYSIS

A Case-Study Approach

Solutions to Selected Problems

Rangaraj M. Rangayyan
"University Professor"
Professor, Department of Electrical and Computer Engineering
Adjunct Professor, Departments of Surgery and Radiology
University of Calgary, 2500 University Drive N.W.
Calgary, Alberta, Canada T2N 1N4
Phone: +1 (403) 220-6745
Fax: +1 (403) 282-6855
e-mail: ranga@ucalgary.ca
Web: http://www.enel.ucalgary.ca/People/Ranga/enel563

Book published by IEEE Press, Piscataway, NJ, 2002
in The IEEE Press Series in Biomedical Engineering
with Wiley Interscience, John Wiley & Sons, Inc., New York, NY

Version: November 29, 2004

Acknowledgments

I thank Sridhar Krishnan, Naga Ravindra Mudigonda, Fábio José Ayres, and Randy Hoang Vu for help in preparing the problems and solutions.

Rangaraj Mandayam Rangayyan
Calgary, Alberta, Canada
November, 2004

Contents

Chapter 1

Solutions to Selected Problems

1. Any two along the lines of the following:

   - EEG analysis in sleep research.
   - EEG monitoring for the detection of seizures and epilepti-form spike activity.
   - Spectrum analysis for the detection of EEG rhythms (α, β, δ, etc.).
   - Analysis of the ECG of critically ill patients for heart-rate monitoring and detection of arrhythmia.

2. Any two along the lines of the following:

   - To investigate and understand physiological phenomena.
   - To detect abnormal or pathological (disease) processes.
   - To perform objective and quantitative analysis of signals for consistent and repeatable interpretation.
   - To provide assistance to physicians and medical specialists in making more accurate diagnostic decisions.

3. In open-loop monitoring, data are acquired from the patient for analysis and interpretation by a medical specialist. There is no direct action taken on the patient. For example, in a common heart-rate monitor, the system simply displays the heart rate. If the heart rate drops below a limit or exceeds a limit, the system may set off alarms, but does not apply any remedial procedures to the patient directly.

In closed-loop monitoring, the results of data analysis are used to respond to the conditions detected by performing some action on the patient. For example, a combined defibrillator-pacemaker can detect when ventricular fibrillation occurs, and apply a defibrillating shock to the heart.

4. Any three along the lines of the following:

- Power-line interference.
- Electromagnetic radiation from nearby equipment, lamps, computers, monitors, etc.
- Motion (EMG) artifact in the ECG due to patient movement, coughing, etc.
- ECG appearing as an artifact in EEG signals.
- Ongoing EEG appearing in event-related potentials.

5. Once a cell has been triggered, it cell cannot be triggered again until the refractory period is completed.

Given that the total action potential duration of the cell is 10 ms, including the refractory period, the cell may be triggered every 10 ms, or at a maximum rate of 100 times per second.

6. The cell cannot be triggered again within the duration of an action potential, including the refractory period. The highest possible rate is to trigger the cell every 300 ms. Then, the maximum rate is $\frac{1}{0.300} = 3.33$ times per second, or $\frac{60 \times 1{,}000}{300} = 200$ times per minute.

7. Spatial recruitment: more and more motor units of the same muscle are recruited into contraction in order to increase the total output power of the muscle.

Temporal recruitment: the motor units that are already active are triggered more often into contraction; that is, the firing rate is increased, in order to increase the total output power of the muscle.

8. See Figure 1.1.

Temporal recruitment: the firing rates of the motor units that have already been recruited into action are increased to obtain more force.

Spatial recruitment: new motor units are brought into action to increase the output force.

Spatio-temporal recruitment: combination of the above two.

9. See Figure 1.2.

10. See Figure 1.3.

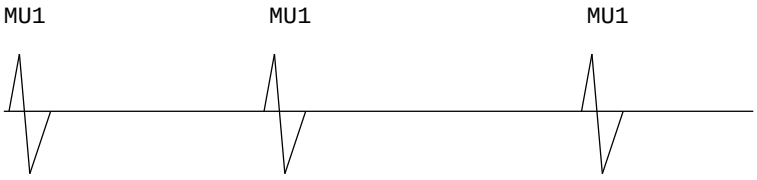

(a) At the beginning:
only MU1 is firing at a low rate

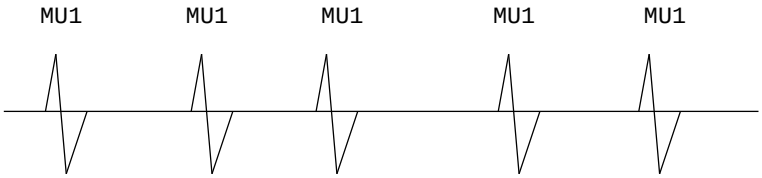

(b) A little later: with temporal recruitment, the
firing rate of MU1 is increased. No other MU recruited yet.

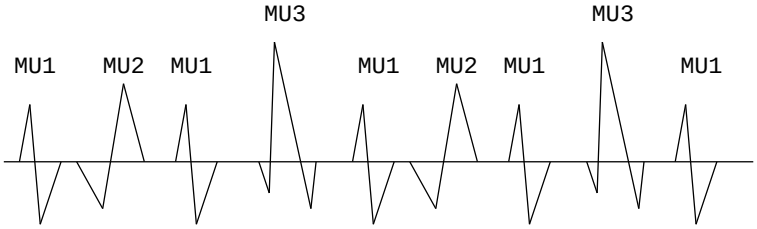

(c) A little later: with spatial recruitment, new motor
units MU2 and MU3 have been brought into action. MU1
continues to fire at the same rate as in (b).

Figure 1.1: Problem 1.8: EMG from three active motor units (MUs), demonstrating spatial and temporal recruitment. Each signal frame represents a time interval of about 500 ms. More MUs are recruited and the firing rates of the active MUs increase as the level of contraction increases, from the condition in (a) to (b) to (c).

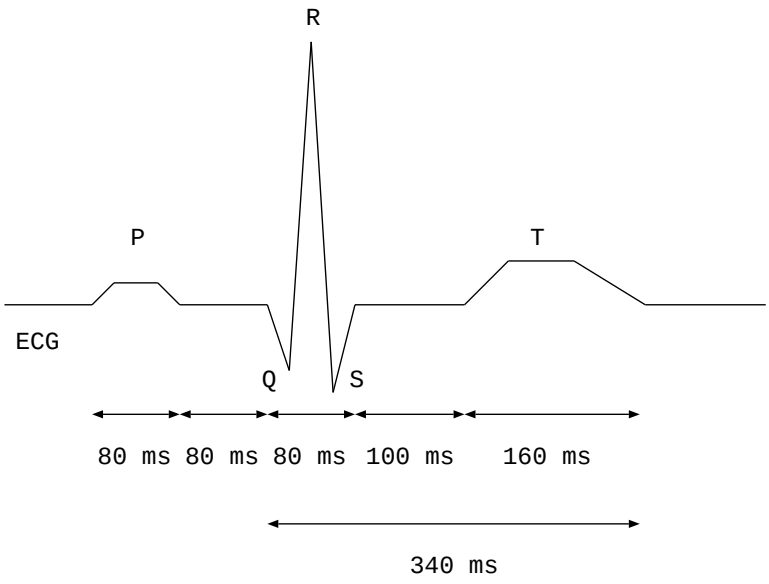

just before P: SA node fires

P: atrial depolarization or contraction

PQ: AV node delay; atrial repolarization

just before Q: AV node fires

QRS: ventricular depolarization or contraction (systole)

ST: plateau phase of ventricular myocyte action potential

T: ventricular repolarization

after T: ventricular relaxation (diastole)

Figure 1.2: Problem 1.9: A typical normal ECG signal over one cardiac cycle.

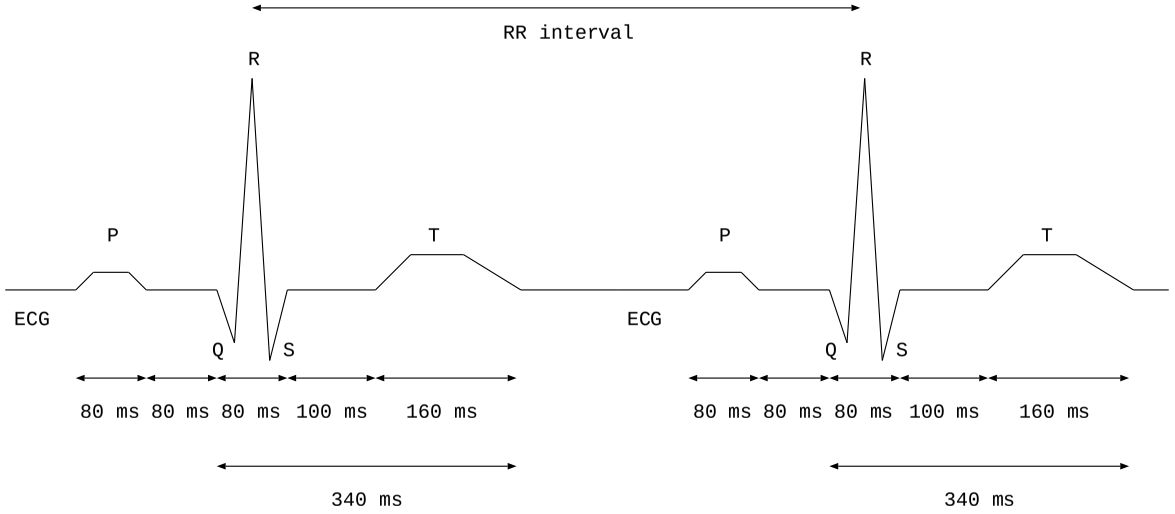

P: atrial depolarization or contraction

PQ: atrial repolarization
(atrial relaxation continues until the next P wave)

QRS: ventricular depolarization or contraction (systole)

T: ventricular repolarization; ventricular relaxation (diastole)
continues until the next QRS wave.

Figure 1.3: Problem 1.10: A typical normal ECG signal over two cardiac cycles.

11. The P wave relates to the contraction of the atria. This process is a slow, squeezing action. The atria do not possess specialized conducting nerve fibers; instead, the activation process propagates through the muscle fibers. This results is slow propagation and activation of the atrial muscles. Furthermore, the action potential of atrial muscle fibers has a short duration of the order of $150 - 200\ ms$. For these reasons, the P wave is a relatively slow and smooth (low-frequency) wave.

The QRS wave relates to the contraction of the ventricles. Due to the rapid conduction of the activation signals rapidly through the bundle branches and the Purkinje fibers, the ventricular muscles are activated in a rapid sequence. Furthermore, the action potential of ventricular myocytes is of a relatively long duration of about $300 - 350\ ms$. For these reasons, the QRS is a sharp (high-frequency) wave.

The T wave relates to the final phase of repolarization of ventricular myocytes, which involves a slow transition from the depolarized state to the polarized state. This phase is much slower than the upstroke of depolarization. Hence, the T wave is a slow and smooth (low-frequency) wave.

See Figure 1.4 for an illustration.

12. The width of the QRS complex is related to the rate of excitation (triggering) of the muscles of the ventricles. Conditions such as bundle-branch block or slow conduction of the excitation pulse through the His bundles and the Purkinje fibers could lead to the widening of the QRS complex to a duration that is greater than the normal value of about $80\ ms$. Ventricular hypertrophy (enlargement) could also cause a wider-than-normal QRS complex.

13. Any two along the lines of the following:

- Analysis of the ECG of critically ill patients for heart-rate monitoring and detection of arrhythmia.
- Analysis of heart-rate variability over time.
- Detection of ectopic beats over a long period of time.
- Accurate measurement of QRS duration, RR interval, etc.
- Filtering to remove power-line interference, high-frequency noise, baseline drift, etc.

14. See Figure 1.5.

Let us assume that the ectopic focus is on the left ventricle.

The ectopic impulse at $1.3\ s$ has no effect because the SA-node excitation has already started the contraction of the ventricles. The same applies to the ectopic impulse at $7.25\ s$. In these two cases, the normal ECG beats result, and the ectopic impulses have no effect.

The ectopic impulse at $2.8\ s$ causes ventricular contraction before the SA-node impulse at $3\ s$. Therefore, a premature ventricular contraction (PVC)

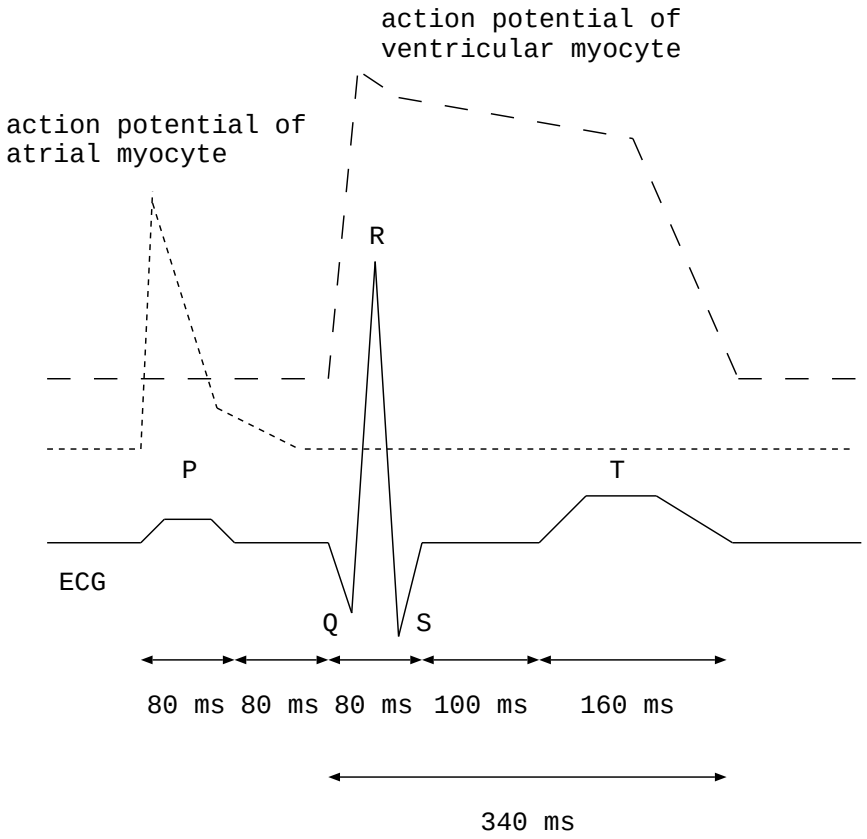

Figure 1.4: Problem 1.11: A typical normal ECG signal over one cardiac cycle. The typical action potentials of an atrial myocyte and a ventricular myocyte are also shown.

results. The P wave due to the SA-node impulse is buried in the PVC. A regular QRS wave is not observed in the ECG.

The SA-node impulse at 6 s causes a regular P wave in the ECG. A normal QRS wave (ventricular contraction) would have commenced at about ($6 + 0.08$ s for the atrial contraction or P wave $+ 0.08$ s for the PQ interval or the AV-node delay) $= 6.16$ s. However, the ectopic impulse at 6.08 s triggers a PVC. The SA-node impulse has no effect on the ventricles in this case.

15. SA node firing rate $= 80$ bpm.

Interval between SA-node impulses = normal RR interval $= \frac{60 \times 1{,}000}{80} = 750$ ms.

The ectopic focus fires 100 ms before the SA node; therefore, the interval between a PVC and the preceding QRS is $750 - 100 = 650$ ms.

The interval from a PVC to the next normal QRS complex is $2 \times 750 - 650 = 850$ ms.

Due to bigeminy, the patient has an ECG where every normal beat is followed by a PVC, and every PVC is followed by a normal beat including the compensatory pause; see Figure 1.6. Therefore, in an ECG signal with 10 beats, there will be five normal beats with the preceding RR interval of 850 ms including the compensatory pause related to the preceding PVC, and there will be five PVCs with the preceding RR interval of 650 ms due to premature firing by the ectopic focus. The RR histogram will have two values: five for 650 ms and five for 850 ms; see Figure 1.6.

The average RR interval over the 10 beats is $\frac{5 \times 650 + 5 \times 850}{10} = 750$ ms.

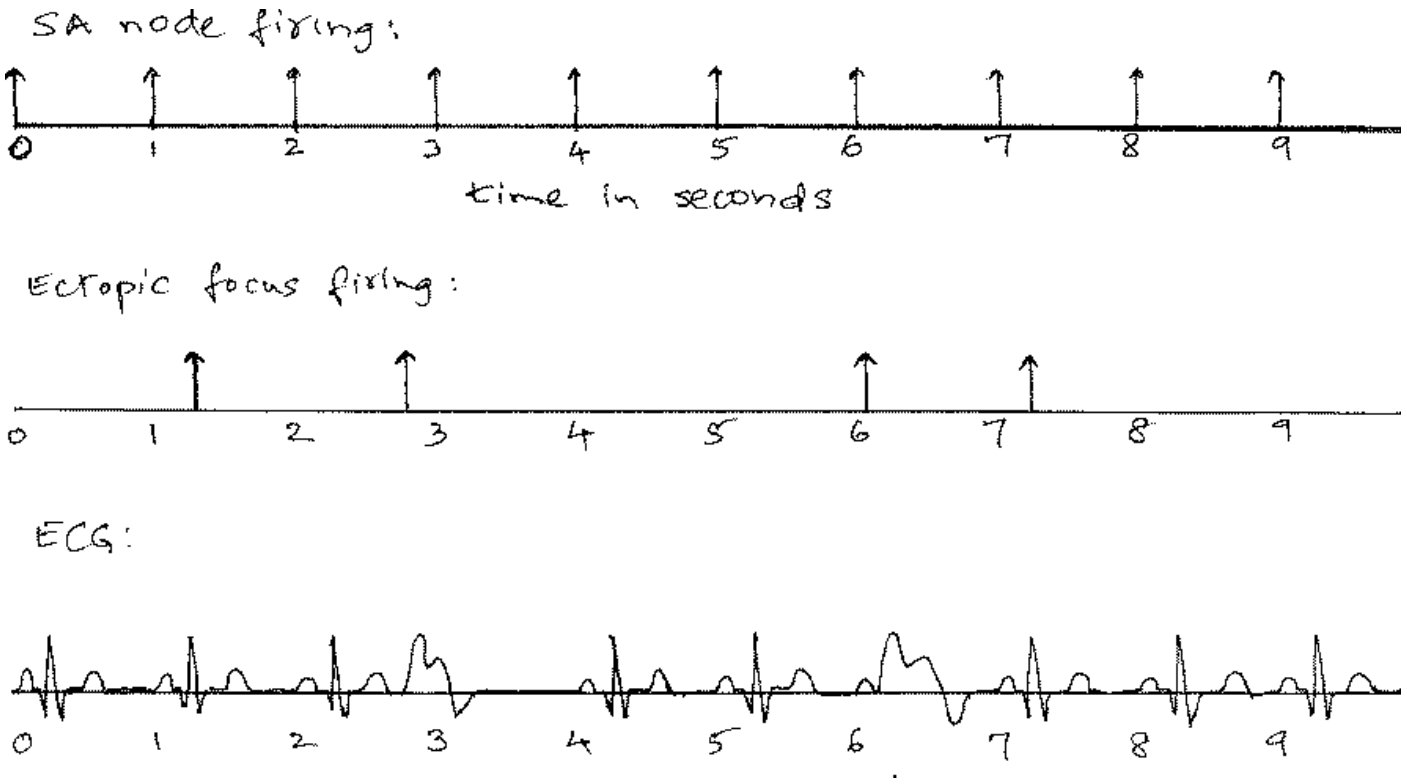

Figure 1.5: Problem 1.14: Regular and ectopic beats caused by the firing of the SA node and an ectopic focus.

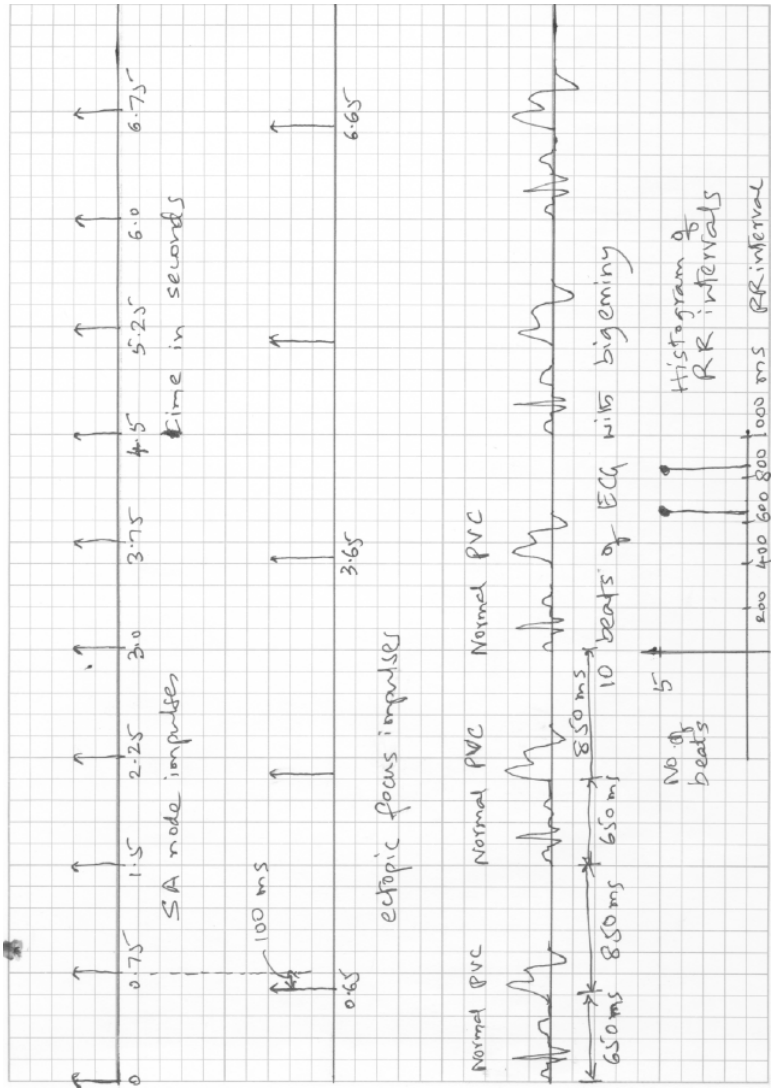

Figure 1.6: Problem 1.15: The ECG of a patient with bigeminy.

16. See Figure 1.7.

S1: The first heart sound (S1) occurs at the beginning of ventricular contraction (systole). This corresponds to the QRS wave in the ECG. At the beginning of S1, the atrioventricular (AV) valves (mitral and tricuspid) close. The deceleration of the blood causes some vibrations and sounds. After the isovolumic part of the contraction of the ventricles (with all of the four valves closed), the semilunar (aortic and pulmonary) valves open. The blood is then ejected out of the ventricles into the aorta and the pulmonary artery. This causes vibrations due to the acceleration of and turbulence in the ejected blood.

The duration of S1 is about $100 - 150\ ms$.

S2: At the end of systole, the aortic and pulmonary valves close. The deceleration of the blood causes some vibrations and sounds. S2 usually has two distinct components related to the closure of the aortic valve (A2) and the closure of the pulmonary valve (P2).

The duration of S2 is about $80 - 100\ ms$.

Sometimes, the third and fourth heart sounds (S3 and S4) could be heard; they are not considered in this example.

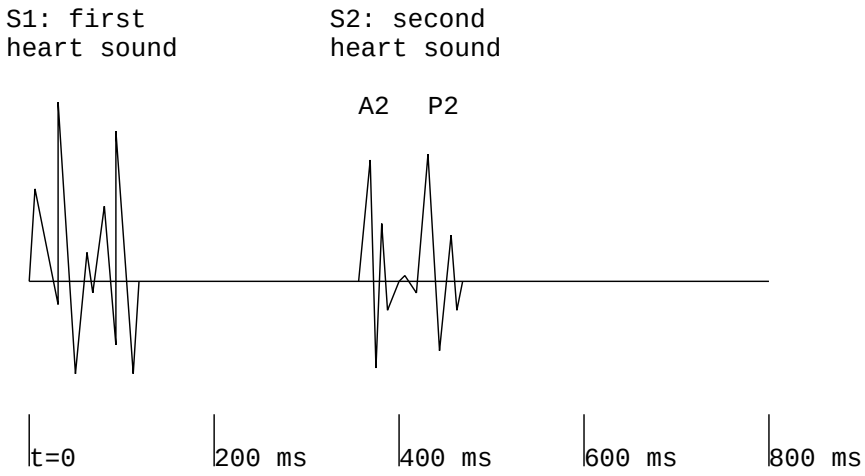

Figure 1.7: Problem 1.16: A typical normal PCG signal over one cardiac cycle.

17. Any two along the following lines:

- Monitoring of the various stages of sleep (delta and theta waves).
- Detection of epileptic seizures and related waves (sharp waves, spike-and-wave complexes).

- Biofeedback for relaxation and the treatment of hyper-anxiety.

18. The term "rhythm" in the context of the ECG refers to the rhythm of the heart (cardiac activity). Cardiac rhythm is expressed in terms of beats per minute (bpm), assuming a nearly constant RR interval. Bradycardia represents a low heart rate of less than 60 bpm, whereas tachycardia represents a high heart rate of greater than 120 bpm. The presence of PVCs or significant variations in the RR interval indicate cardiac arrhythmia.

In the context of the EEG, the term "rhythm" represents the dominant frequency of the EEG wave. For example, we have the alpha rhythm indicating a dominant frequency in the range $8 - 13$ Hz, the beta rhythm indicating a dominant frequency that is greater than 13 Hz, and the theta rhythm indicating a dominant frequency in the range $4 - 8$ Hz. The EEG rhythms relate to the level or nature of the activity of the brain, with alpha representing a wakeful but relaxed state with no external stimuli; beta representing a high level of mental activity, tension, or anxiety; and theta indicating the early stages of sleep.

Chapter 2

Solutions to Selected Problems

None.

Chapter 3

Solutions to Selected Problems

1. Sources of instrumentation artifacts in recording the PCG signal:

   - High-frequency noise (ambient EM waves) picked up by cables.
   - Power-line (60 Hz) interference from the system.
   - External sounds and vibrations picked up by the transducer.

Sources of physiological artifacts in recording the PCG signal and nonelectronic methods to prevent or minimize the artifacts:

   - Breath sounds. May be prevented if the subject can hold breath during the recording period.
   - Bowel sounds due to peristalsis and gas. Difficult to prevent; the patient may be requested to come with an empty stomach.
   - Movement artifact. May be prevented if the subject can remain relaxed and still.

2. Any four along the lines of the following:

   Instrumentation artifacts:

   A. White noise or high-frequency noise due to electronic (or thermal) noise in amplifiers and filters. May be removed by lowpass filtering to about 70 Hz.

   B. Power-line artifact picked up through cables or due to poor grounding of the equipment. May be removed by notch or comb filtering.

C. Broad-band electromagnetic noise picked up from the surroundings due to poor shielding of cables. May be prevented by good shielding of the cables. May be removed by lowpass filtering to about 70 Hz.

D. Low-frequency artifact due to lack of firm contact of the electrodes with the skin. May be prevented by firmly attaching the electrodes with adequate conducting gel. May be removed by highpass filtering with a cutoff of about 0.05 Hz.

Physiological artifacts:

A. EMG due to tight muscles, coughing, squirming, etc. May be prevented by getting the subject to relax all limb and chest muscles, and to stop breathing for the duration of the recording.

B. EMG and baseline drift due to breathing (causing variable contact with chest electrodes). May be prevented by getting the subject to stop breathing for the duration of the recording. The high-frequency components of the ECG may be removed by lowpass filtering to about 70 Hz. Baseline drift may be removed by highpass filtering with a cutoff of about 0.05 Hz.

3. Potential sources of physiological artifacts in recording the EEG:

- The ECG appearing in the EEG.
- EMG due to tense scalp muscles.
- EMG due to pulsatile movement of blood in the arteries of the brain.
- EMG due to movement of the eyes, forehead, or head.
- Event-related potentials related to various stimuli (ambient lights and sounds) that may not be desired in the EEG.

4. n/a.

5. (a) $2 \times 150 = 300\ Hz$.
(b) See Figure 3.1 (a).
(c) See Figure 3.1 (b).
There is no aliasing error with $f_s = 500\ Hz$. In the case of $f_s = 200\ Hz$, the frequency components in the range $100 - 150\ Hz$ are aliased into the band $50 - 100\ Hz$. Therefore, the components of the signal in the range $50 - 150\ Hz$ are corrupted due to aliasing errors.

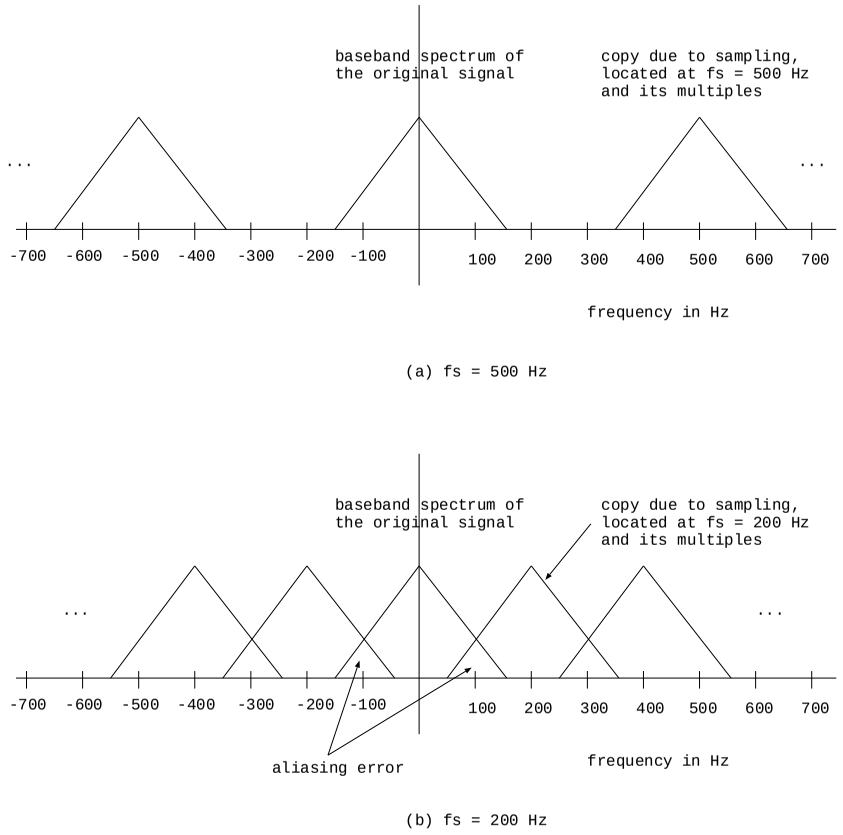

Figure 3.1: Problem 3.5: (a) Spectrum of a signal that is bandlimited to $0 - 150\ Hz$, after sampling at $500\ Hz$. (b) Spectrum of a signal that is bandlimited to $0 - 150\ Hz$, after sampling at $200\ Hz$.

Figure 3.2: Problem 3.5*: (a) Spectrum of a signal that is bandlimited to $0-200\ Hz$, after sampling at $1,000\ Hz$. (b) Spectrum of a signal that is bandlimited to $0-200\ Hz$, after sampling at $300\ Hz$.

5*. The same as Problem 3.5, but with the bandwidth changed to 200 Hz, the first sampling rate changed to $1,000$ Hz, and the second sampling rate changed to 300 Hz.

(a) $2 \times 200 = 400$ Hz.

(b) See Figure 3.2 (a).

(c) See Figure 3.2 (b).

There is no aliasing error with $f_s = 1,000$ Hz. In the case of $f_s = 300$ Hz, all components above 150 Hz are aliased, and the frequency components in the range $100 - 200$ Hz are corrupted due to aliasing errors. For example, the aliased version of the component at 190 Hz gets added to the true component at 110 Hz.

6. Ensemble averages are computed by using a collection (ensemble) of signals of the same nature. Averaging is performed across multiple signals.

Temporal (time) averages are computed for a single signal (or for each signal individually) by using collections of samples at various instants of time or a moving window of samples along the time axis.

The mean is a first-order average. The mean of an EEG signal, at a given instant of time over an ensemble or over all time for a single channel, has no practical use because most signals are acquired as differential signals between two locations on the scalp; the mean of such signals is usually zero. However, weighted temporal means in a moving window can be used to filter an EEG signal for the removal of noise. Furthermore, synchronized averaging across a collection (ensemble) of event-related potentials performed over the expected duration of the response is useful in reducing noise and increasing the SNR.

The autocorrelation function (ACF) is a second-order average. The ACF is useful in detecting periodic or repeated appearances of patterns such as spike-and-wave complexes, as well as in detecting EEG rhythms such as the alpha wave.

The variance is useful as an estimate of the power of the signal, which could be used in determining the SNR.

7. n/a.

8. (a) The ECG is a quasi-periodic signal: repeated cycles (P-QRS-T waves) appear at almost regular intervals. If we assume that the noise affecting the signal is independent from one cardiac cycle to another, we could segment each cycle of the ECG and average several such cycles to reduce noise.

(i) Synchronization could be achieved by detecting the QRS complex of each beat (by, for example, template matching) and segmenting a cardiac cycle by selecting a starting point that is about $200 - 250$ ms before the QRS point detected (in order to include the P wave), and an ending point that is about $350 - 400$ ms after the QRS point detected (in order to include the T wave).

(ii) Artifacts could arise if the ECG waveshape varies from beat to beat or if PVCs arise. A PVC-detection algorithm could be used to reject cardiac cycles related to PVCs. Artifacts also arise if the baseline drifts during the averaging

period.

(iii) A limitation of this method is that the result will be the ECG over one cardiac cycle only.

(iv) The potential for success is good, with the limitations mentioned above.

(b) Event-related potentials (ERPs) are obtained under repeated stimulation of the system of interest. For example, visual ERPs are obtained by the repeated application of a flash signal (strobe light).

(i) Because the stimulus is applied under the experimenter's control, the exact instant for synchronization is known.

(ii) Power-line artifact may be suppressed by repeating the stimuli at a rate that does not relate to the power-line frequency, such as 1.7 times per second. The patient's EEG could interfere with the ERPs; this may be controlled by getting the patient to relax, and by ensuring that no other external stimuli (lights or sounds) are presented to the subject during the experiment.

(iii) The system being stimulated may or may not produce the same response to every stimulus. Variations from one response to another could smear or blur the details of interest in the averaged ERP. The application of a large number of stimuli could lead to fatigue and habituation, which could lead to changes in the ERP and a poor averaged result.

(iv) The potential for success is excellent, with the limitations mentioned above.

(c) Like the ECG, the PCG is also a quasi-periodic signal. However, the PCG exhibits noticeable variation from one cardiac cycle to the next due to the random nature of the vibration signals. (The effects of breathing and chest-wall movement could be controlled by having the patient hold breath during the recording period.) For this reason, direct averaging of the PCG signal may lead to cancellation of the vibration waveforms! However, the envelope and power spectral density (PSD) of the PCG may be computed for each segmented sound component (such as S1, systolic murmur, S2, and diastolic murmur). Because the envelope and the PSD are nonnegative functions, they may be averaged over multiple cardiac cycles to obtain averaged estimates of the functions.

(i) The QRS complex of the ECG may be detected and used as a trigger, as described under part (a). However, this signal can only give a reliable indicator of the beginning of S1. The dicrotic notch in the carotid pulse signal may be detected and used to determine the beginning of S2. A test of randomness could be used to determine the end of S1 or S2 and the corresponding beginning points of systolic or diastolic murmur, if present.

(ii) The effects of breathing and chest-wall movement should be controlled by having the patient hold breath during the recording period. As in the case of the ECG, cardiac cycles related to PVCs should be detected and rejected.

(iii) The PCG signal exhibits more variability from beat to beat due to the random nature of vibrations. For this reason, averaging would be desired over a large number of cardiac cycles to remove inter-beat variation. Variations in the heart rate during the recording and averaging period could cause significant variations in the duration of the diastolic segment: we could have a fixed point

for the beginning of the diastolic segment, but allow the duration or the end point to vary from one segment to another.

(iv) The potential for success is good, with the limitations mentioned above. The method cannot provide an averaged PCG signal, but only an averaged envelope or PSD.

(d) The surface EMG signal is an almost-random signal due to the superposition of a large number of motor-unit action potentials (MUAPs). For this reason, averaging of the surface EMG signal itself is not feasible: the result may tend to zero! However, measures derived from the surface EMG, such as its envelope and RMS value, could be averaged over multiple acquisitions.

Single-motor-unit action potentials (SMUAPs) segmented from needle EMGs may be aligned and averaged to reduce noise. However, no reference would be available for such segmentation.

(i) Synchronization of the signal segments is not required, as long as all of the acquisitions relate to the same level of activity of the same muscle. In the case of quasi-periodic activities such as breathing, the nasal airflow or temperature may be used to detect the beginning of each breath.

(ii) The EMG signal may be highpass filtered to remove low-frequency artifact and power-line artifact. The computed parameters as mentioned above may not be susceptible to other artifacts.

(iii) Fatigue could affect the signals acquired after several repetitions of muscular activity. Adequate rest between repetitions should minimize this effect.

(iv) Fair, with the note that the averaging procedure may be applied only to computed functions and parameters such as the envelope and RMS value, and not to the EMG signal directly.

9. n/a.

10. $X(z) = \sum_{n=0}^{N} x(n)\, z^{-n}$

    Given $x(0) = 4$, $x(1) = 3$, $x(2) = 2$, etc.

    $X(z) = 4 + 3z^{-1} + 2z^{-2} + z^{-3} - z^{-5} + z^{-7}$.

11. (a) See Figure 3.3 (a).
    (b) See Figure 3.3 (b).

12. Given $h(n) = \{2, 1, 0, 0, -1, 0, 1, 0\}$.

    $H(z) = \sum_{n=0}^{N} h(n)\, z^{-n}$

    $H(z) = 2 + z^{-1} - z^{-4} + z^{-6}$.

13. $h(n) = \{1, -2, 1\}$.

    $y(n) = x(n) * h(n) = x(n) - 2x(n-1) + x(n-2)$

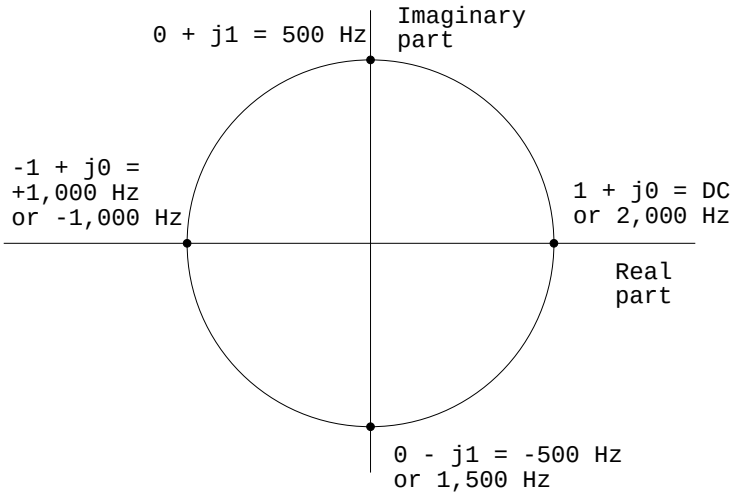

(a) unit circle in the z-plane with fs = 2,000 Hz

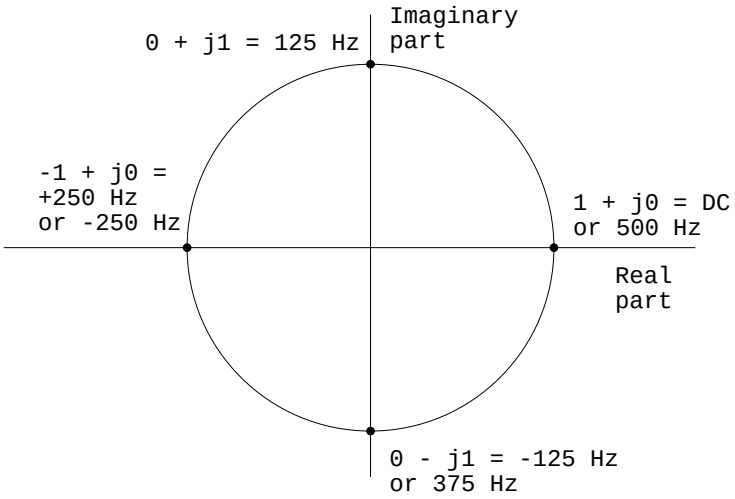

(b) unit circle in the z-plane with fs = 500 Hz

Figure 3.3: Problem 3.11: (a) Unit circle in the z-plane for a signal sampled at $2,000\ Hz$. (b) Unit circle in the z-plane for a signal sampled at $500\ Hz$.

Given that $x(n)$ is the unit step function, we have $x(n) = 0$ for $n < 0$ and $x(n) = 1$ for $n \geq 0$. Then,

$y(0) = x(0) = 1$

$y(1) = x(1) - 2x(0) = 1 - 2 = -1$

$y(2) = x(2) - 2x(1) + x(0) = 1 - 2 + 1 = 0$

$y(3) = x(3) - 2x(2) + x(1) = 1 - 2 + 1 = 0$

$y(n) = 0$ for $n \geq 2$.

See Figure 3.4.

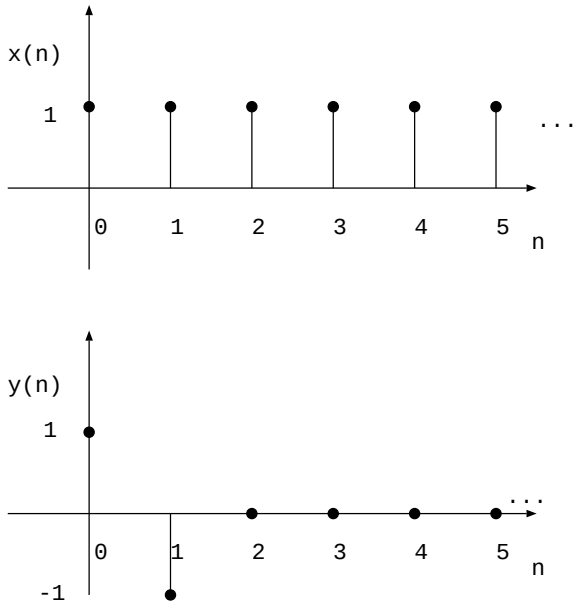

Figure 3.4: Problem 3.13: (a) Unit step function. (b) Response of the filter with $h(n) = \{1, -2, 1\}$ to unit step input.

14. $h(n) = \{3, -2, 2\}$.

$x(n) = \{6, 4, 2, 1\}$.

$y(n) = h(n) * x(n) = \sum_k x(k)\, h(n-k) = \{18, 0, 10, 7, 2, 2, 0, 0, 0\}$.

See Figure 3.5. Observe that the result has a longer duration than either input, equal to the sum of the durations of the two input signals.

15. Given $H(z) = z^{-1} - 3z^{-2} + 2z^{-4} - z^{-6}$.

The difference equation is $y(n) = x(n-1) - 3x(n-2) + 2x(n-4) - x(n-6)$.

The impulse response is the output when the input is the delta function, that is, when $x(n) = \delta(n)$. Thus, we have

$h(n) = \delta(n-1) - 3\delta(n-2) + 2\delta(n-4) - \delta(n-6)$.

See Figure 3.6 for a plot of the impulse response.

16. Given $h(n) = \{3, 2, 1, 0, -1, 0, 0, 1\}$.

Assume that the first sample corresponds to $n = 0$. Then, we have $h(n) = 3\delta(n) + 2\delta(n-1) + \delta(n-2) - \delta(n-4) + \delta(n-7)$.

The transfer is given by the z-transform of $h(n)$, as

$H(z) = 3 + 2z^{-1} + z^{-2} - z^{-4} + z^{-7}$.

17. n/a.

18. See Figure 3.7. Artifacts are present at the fundamental power-line frequency of 60 Hz; at 20 Hz due to the aliasing of the 180 Hz component as $200 - 180 = 20$ Hz; and at 100 Hz due to the aliasing of the 300 Hz component as $400 - 300 = 100$ Hz. Conjugate components will also be present at $-20, -60$, and -100 Hz.

A comb filter with zeros at $20, 60$, and 100 Hz may be used to remove the power-line frequency components (fundamental and the aliased harmonics). Alternatively, a Wiener filter may also be designed, with appropriate specification of the PSDs of the original (desired) signal and the noise (artifact) in the digitized signal.

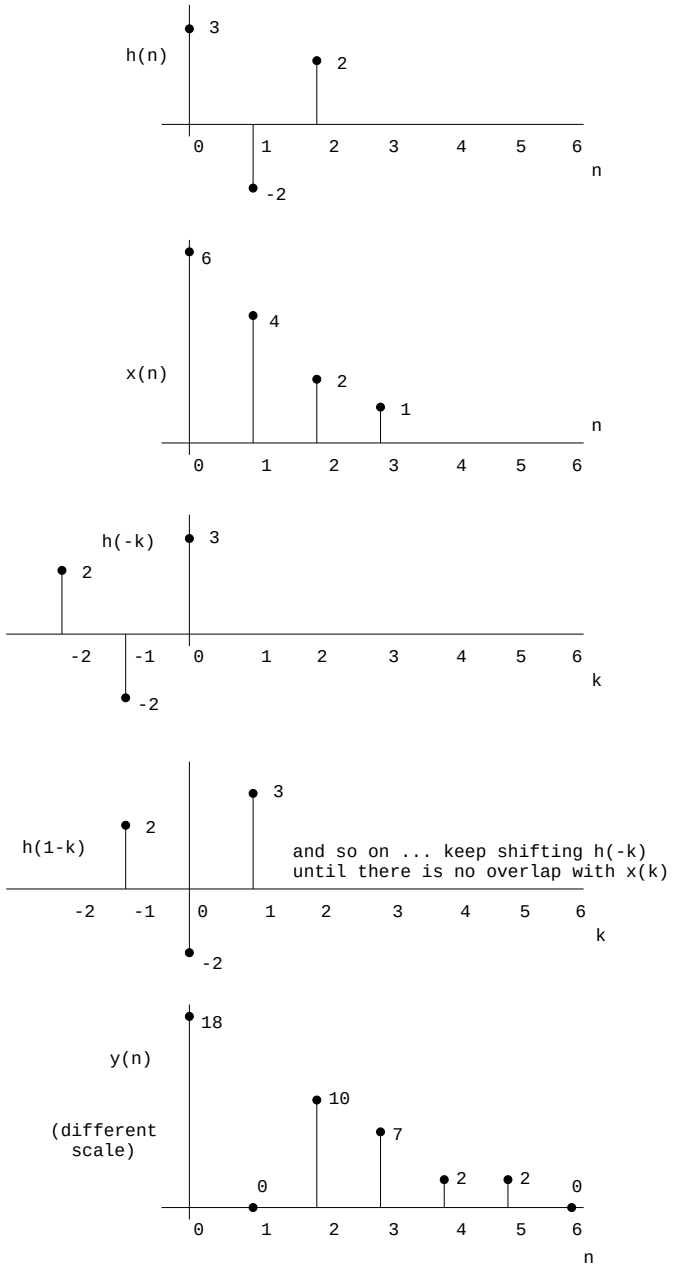

Figure 3.5: Problem 3.14: Example of linear convolution of two signals.

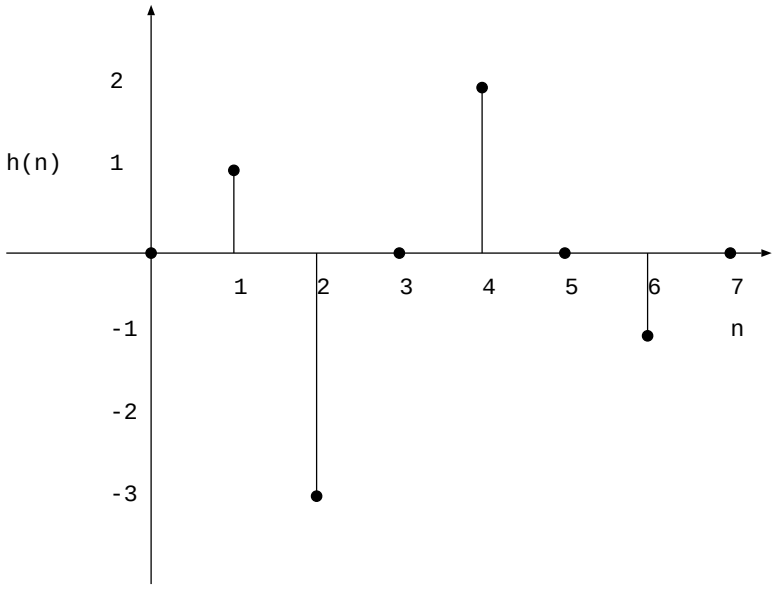

Figure 3.6: Impulse response of the system in Problem 3.15. $h(n) = \delta(n-1) - 3\delta(n-2) + 2\delta(n-4) - \delta(n-6)$.

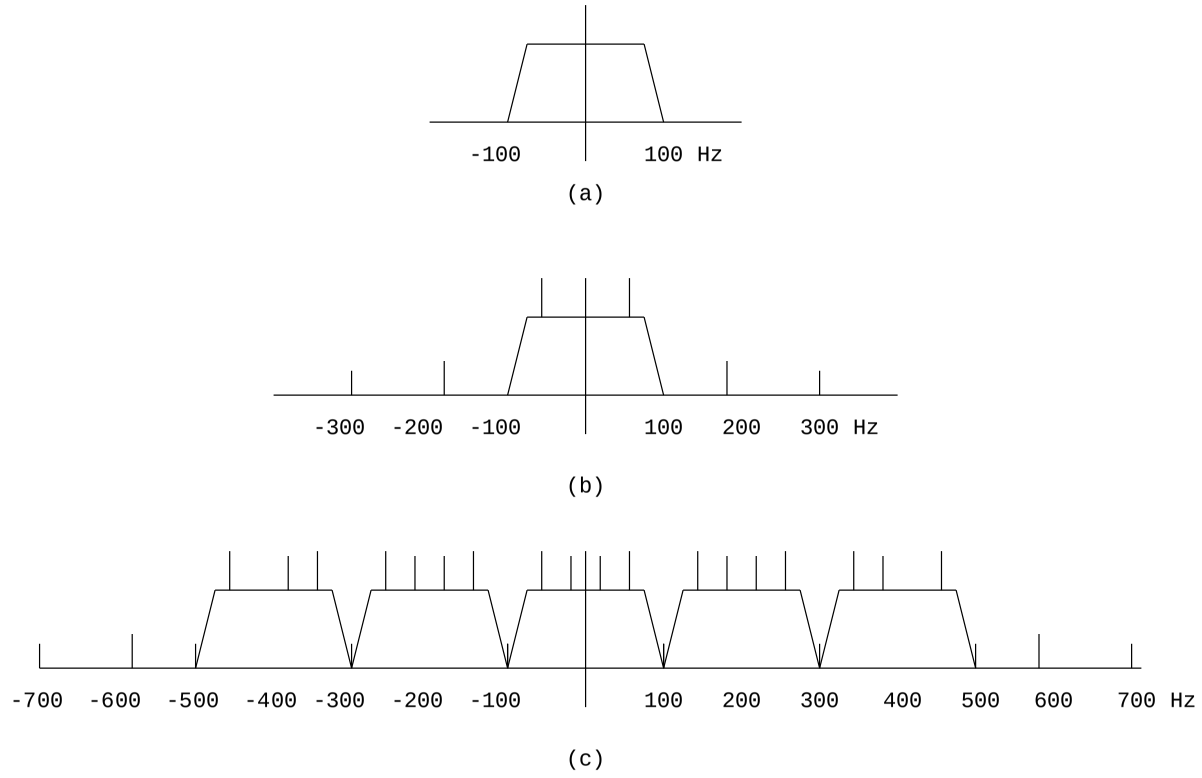

Figure 3.7: Problem 3.18: (a) Spectrum of the biomedical signal. (b) Spectrum of the biomedical signal with the power-line artifact added. (c) Spectrum of the contaminated signal after sampling at 200 Hz. Copies of the spectrum and their effects are shown only for the baseband and center frequencies of ± 200 and ± 400 Hz. Additional aliased components will appear at frequencies > 300 and < -300 Hz when the copies of the signal spectrum are placed at $\pm 600, \pm 800, \ldots,$ Hz.

19. n/a.

20. (a) $H(z) = H_1(z)\,H_2(z)$.

$$\begin{aligned} H(z) &= \frac{1}{3}(1+z^{-1}+z^{-2})(1-z^{-1}) \\ &= \frac{1}{3}(1+z^{-1}+z^{-2}-z^{-1}-z^{-2}-z^{-3}) \\ &= \frac{1}{3}(1-z^{-3}). \end{aligned}$$

(b) Because $H(z) = \sum_{n=0}^{N} h(n)\,z^{-n}$, we have $h(0) = \frac{1}{3}$, $h(1) = 0 = h(2)$, $h(3) = -\frac{1}{3}$, and $h(n) = 0$ for $n > 3$.

(c) DC corresponds to $z = 1$. Therefore, the DC gain is given by $|H(1)| = |\frac{1}{3}(1-1)| = 0$.

The folding frequency $f_s/2$ occurs in the z-plane at $z = -1$. Therefore, the gain is given by

$H(-1) = \frac{1}{3}(1-(-1)^{-3}) = \frac{2}{3}$.

21. Given

$$\begin{aligned} H(z) &= \frac{Y(z)}{X(z)} \\ &= \frac{1+2z^{-1}+z^{-2}}{1-z^{-2}} \\ &= \frac{(1+z^{-1})^2}{(1+z^{-1})(1-z^{-1})} \\ &= \frac{(1+z^{-1})}{(1-z^{-1})}. \end{aligned}$$

(a) Difference equation: $y(n) = x(n) + 2x(n-1) + x(n-2) + y(n-2)$.

(b) and (c): See Figures 3.8 and 3.9.

22. (a)

$$\begin{aligned} H(z) &= G\,\frac{[1-z^{-1}(0.5+j0.5)][1-z^{-1}(0.5-j0.5)]}{[1-z^{-1}(-0.6+j0.3)][1-z^{-1}(-0.6-j0.3)]} \\ &= G\,\frac{1-z^{-1}+0.5\,z^{-2}}{1+1.2\,z^{-1}+0.45\,z^{-2}}, \end{aligned}$$

where G is a gain factor.

(b) $y(n) = G[x(n) - x(n-1) + 0.5\,x(n-2)] - 1.2\,y(n-1) - 0.45\,y(n-2)$.

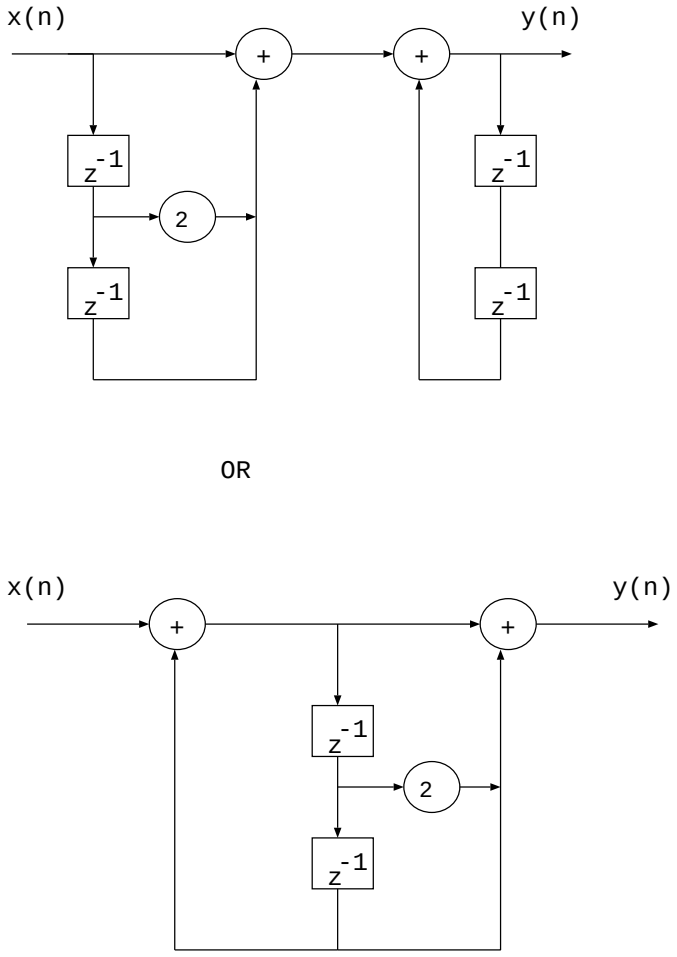

Figure 3.8: Problem 3.21: Two possible signal-flow graphs for the transfer function $H(z) = \frac{Y(z)}{X(z)} = \frac{1+2z^{-1}+z^{-2}}{1-z^{-2}}$.

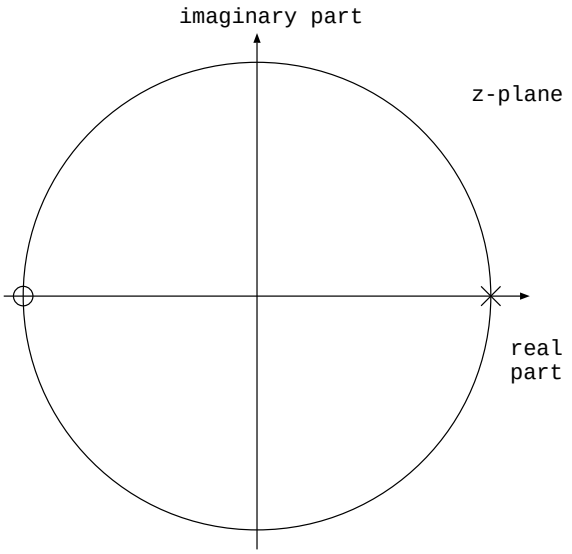

Figure 3.9: Problem 3.21: Pole-zero diagram for the filter with the transfer function $H(z) = \frac{Y(z)}{X(z)} = \frac{1+2z^{-1}+z^{-2}}{1-z^{-2}}$. An extra pole and zero cancel each other at $z = -1$.

(c) The filter has only one pair of poles and one pair of zeros. The maximum gain occurs at or near the frequency of the poles (resonance): the effect of a pole is pronounced when it is located close to the unit circle, and reduced when it is away from the unit circle in the z plane. With the pole at $(-0.6 + j0.3)$, we have the angle of the pole as -26.6^o or 153.4^o. With 360^o corresponding to the sampling frequency of $1,000\ Hz$, we have the frequency of the pole as $426\ Hz$, which is the frequency around which the gain of the filter reaches its maximum. In this example, the gain reaches its maximum at $z = -1$ or $500\ Hz$, which is the point midway between the two (complex-conjugate) poles. See Figure 3.10 for plots of the frequency response (magnitude and phase) of the filter, obtained using the MATLAB "freqz" function.

Similarly, the minimum gain occurs near the frequency of the zeros (null or anti-resonance). With the zero at $(0.5 + j0.5)$, we have the angle of the zero as 45^o, which leads to the frequency of $125\ Hz$ for the point near which the gain of the filter is at its minimum.

The above discussion is qualitative. The presence of multiple poles and zeros will make analysis as above more difficult. The exact points of the global minimum and maximum may be derived by taking the derivatives of $|H(z)|$ or $|H(\omega)|$; this is not expected in the solution to this problem.

Additional notes: The effects of poles and zeros are more pronounced when they are close to the unit circle in the z plane. See Figures 3.11 and 3.12 for illustrations of the frequency response as the poles and zeros in the given problem are moved closer to the unit circle (indicated by the change in the

magnitude of the poles and zeros; the angles or frequencies are unchanged).

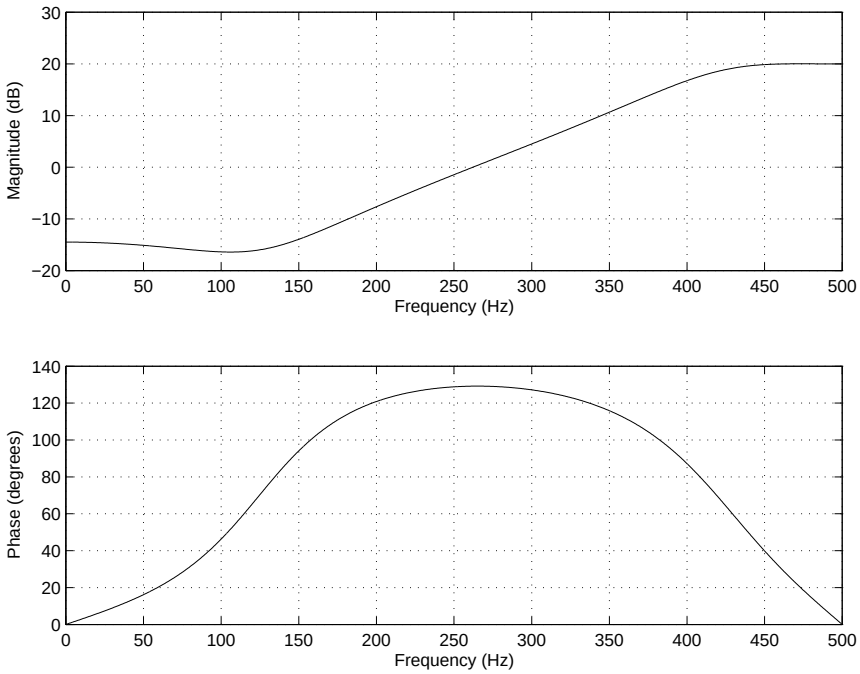

Figure 3.10: Problem 3.22: Frequency response (magnitude and phase) of the filter with poles at $(-0.6 \pm j0.3) = 0.45\angle 153.4^o$ and zeros at $(0.5 \pm j0.5) = 0.7071\angle 45^o$, with the sampling frequency of $1,000\ Hz$.

23. n/a.

24. (a) $Y(z) = z^{-1}\,Y(z) + \frac{1}{4}\,X(z) - \frac{1}{4}\,z^{-4}\,X(z)$

$$\begin{aligned} H(z) &= \frac{Y(z)}{X(z)} \\ &= \frac{1}{4}\,\frac{1-z^{-4}}{1-z^{-1}} \\ &= \frac{1}{4}\,(1+z^{-1})(1+z^{-2}) \\ &= \frac{1}{4}\,(1+z^{-1}+z^{-2}+z^{-3}). \end{aligned}$$

(b) See Figure 3.13.
(c) See Figure 3.14.

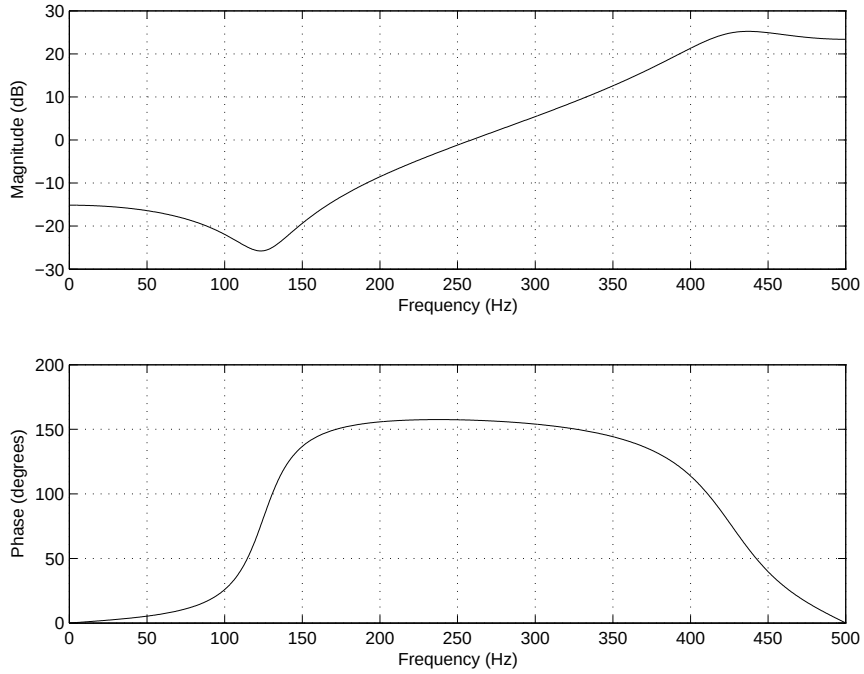

Figure 3.11: Problem 3.22: Frequency response (magnitude and phase) of the filter with poles at $(-0.7156 \pm j0.3577) = 0.8\angle 153.4^o$ and zeros at $(0.6364 \pm j0.6364) = 0.9\angle 45^o$, with the sampling frequency of $1,000\ Hz$.

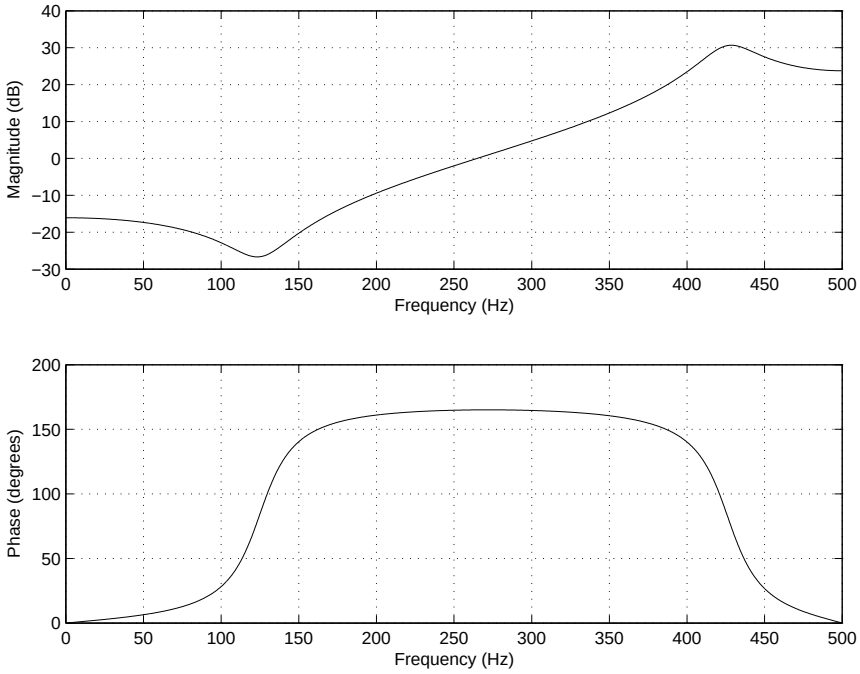

Figure 3.12: Problem 3.22: Frequency response (magnitude and phase) of the filter with poles at $(-0.805 \pm j0.4025) = 0.9\angle 153.4^o$ and zeros at $(0.6364 \pm j0.6364) = 0.9\angle 45^o$, with the sampling frequency of $1,000\ Hz$.

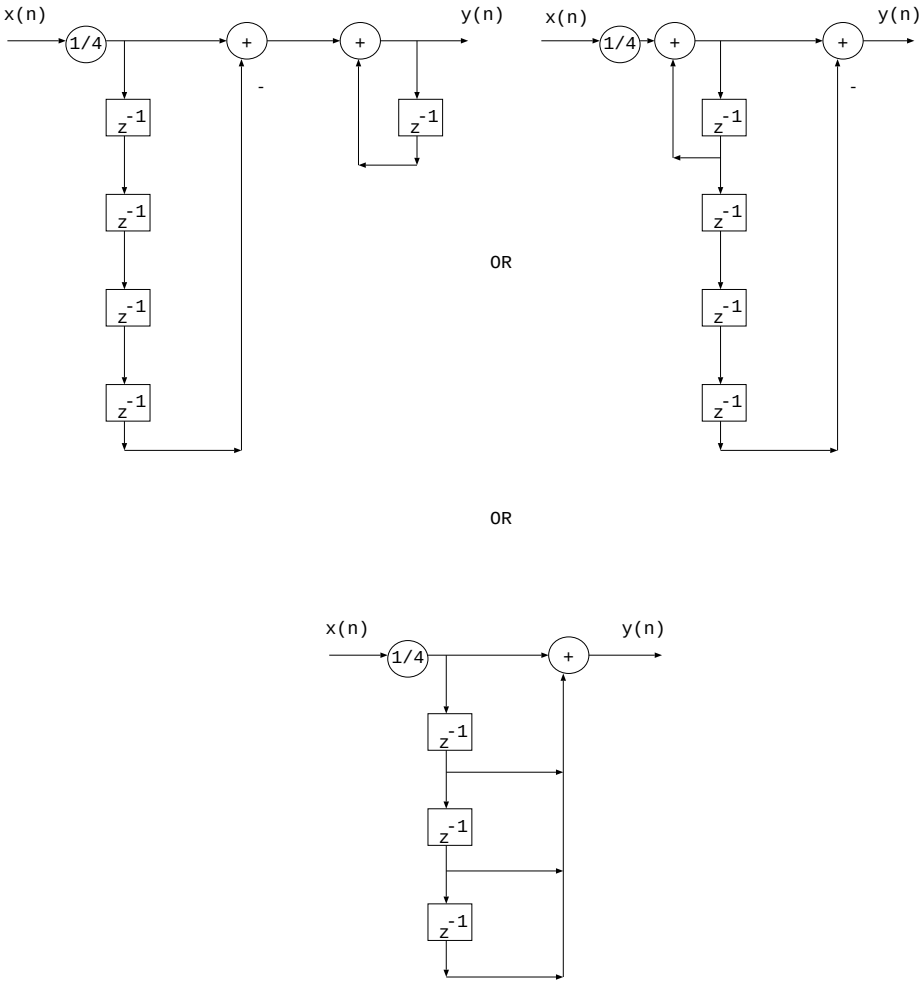

Figure 3.13: Signal flow graph for Problem 3.24.

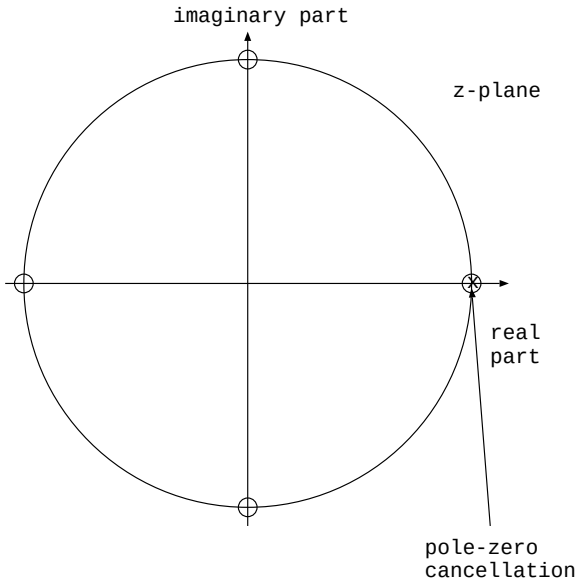

Figure 3.14: Pole-zero plot for Problem 3.24.

25. n/a.

26. Given $x(n) = \{0, 10, 0, -5, 0\}\ mV$; sampling frequency $f_s = 100\ Hz$.
The sampling interval is $T = \frac{1}{f_s} = 10\ mS$.
Given $H(z) = \frac{1}{T}(1 - z^{-1}) = 100(1 - z^{-1})$.
The impulse response of the filter is obtained as the inverse z transform of $H(z)$:
$h(n) = \{100, -100\}$ or $100\,\delta(n) - 100\,\delta(n-1)$.
The output may be obtained by convolving the two sequences for $x(n)$ and $h(n)$, or by applying the difference equation of the filter as follows:
$y(n) = 100x(n) - 100x(n-1)$.
See Figure 3.15 for plots of $x(n), h(n)$, and $y(n)$.

27 – 33. n/a.

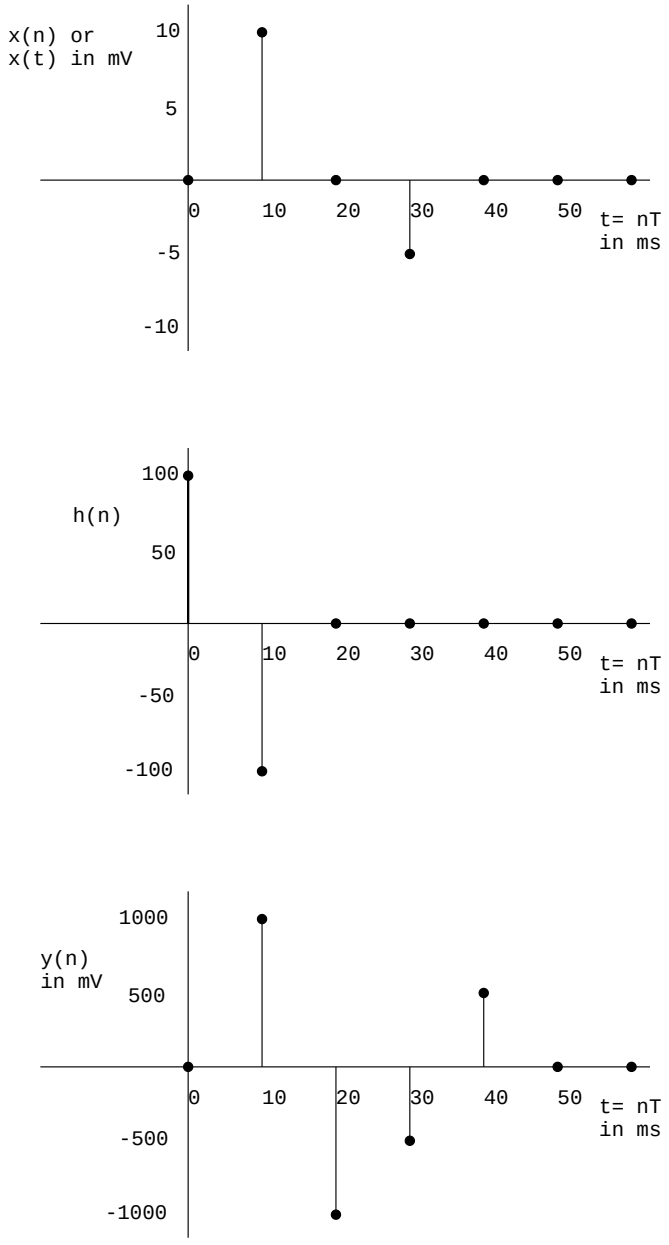

Figure 3.15: The functions $x(n), h(n)$, and $y(n)$ for Problem 3.26. The vertical axis of each plot has a different scale.

Chapter 4

Solutions to Selected Problems

1. By definition, we have the ACF given by

$$\phi_{xx}(\tau) = E[x(t+\tau)x(t)].$$

Now, let us consider the following:

$$E[\{x(t+\tau) \pm x(t)\}^2] \quad \geq \quad 0,$$

because we are taking an average of a positive (or non-negative) expression. It follows that

$$\begin{aligned} E[x^2(t+\tau)] \pm 2E[x(t+\tau)x(t)] + E[x^2(t)] &\geq 0. \\ \phi_{xx}(0) \pm 2\phi_{xx}(\tau) + \phi_{xx}(0) &\geq 0. \end{aligned}$$

Observe that $E[x^2(t+\tau)] = E[x(t+\tau)x(t+\tau)] = \phi_{xx}(0)$. Similarly, $E[x^2(t)] = E[x(t)x(t)] = \phi_{xx}(0)$. The delay between the two time instants considered in each case is zero. Therefore, we have

$$\begin{aligned} 2\phi_{xx}(0) &\geq \mp 2\phi_{xx}(\tau). \\ \phi_{xx}(0) &\geq \mp \phi_{xx}(\tau). \\ |\phi_{xx}(\tau)| &\leq |\phi_{xx}(0)|. \end{aligned}$$

Therefore, the ACF is maximum at $\tau = 0$.

2. *Proof 1:* According to the temporal definition of the ACF of a given signal $x(t)$, we have

$$\phi_{xx}(\tau) = \int_{-\infty}^{\infty} x(t+\tau)x(t)dt. \tag{4.1}$$

Because the process is stationary, this is valid for all t; in other words, the ACF is unaffected by a change in the time origin. Let us now change $t+\tau$ to

a new variable t_1. Then, $t = t_1 - \tau$; $dt = dt_1$; as $t \to \infty, t_1 \to \infty$; and, as $t \to -\infty, t_1 \to -\infty$. Note that τ is a constant as far as the integration with respect to t is concerned.

Then, we have

$$\begin{aligned}\phi_{xx}(\tau) &= \int_{-\infty}^{\infty} x(t_1)x(t_1-\tau)dt_1 \\ &= \int_{-\infty}^{\infty} x(t_1-\tau)x(t_1)dt_1 \\ &= \phi_{xx}(-\tau),\end{aligned}$$

by comparing the last integral above with that in Equation 4.1. Therefore, the ACF is even symmetric.

Proof 2: According to the ensemble average definition, we have the ACF given by

$$\phi_{xx}(\tau) = E[x(t)x(t+\tau)].$$

Similarly, we have

$$\phi_{xx}(-\tau) = E[x(t)x(t-\tau)].$$

Because the process is stationary, the ACF is unaffected by a change in the time origin. Let us now add a shift of τ to t; that is, let us change t to $t+\tau$. Then, we have

$$\begin{aligned}\phi_{xx}(-\tau) &= E[x(t+\tau)x(t+\tau-\tau)] \\ &= E[x(t+\tau)x(t)] \\ &= \phi_{xx}(\tau).\end{aligned}$$

Therefore, the ACF is even symmetric.

3. According to the temporal definition of the ACF of a given signal $x(t)$, we have

$$\phi_{xx}(\tau) = \int_{-\infty}^{\infty} x(t+\tau)x(t)dt.$$

$$\begin{aligned}FT[\phi_{xx}(\tau)] &= \int_{-\infty}^{\infty} \phi_{xx}(\tau)\exp[-j\omega\tau]d\tau \\ &= \int_{-\infty}^{\infty}\left[\int_{-\infty}^{\infty} x(t)x(t+\tau)dt\right]\exp[-j\omega\tau]d\tau \\ &= \int_{-\infty}^{\infty} x(t)\left[\int_{-\infty}^{\infty} x(t+\tau)\exp[-j\omega\tau]d\tau\right]dt.\end{aligned}$$

Now, let $t' = t+\tau$. Then, $\tau = t'-t$, $d\tau = dt'$, and we have the following:

$$FT[\phi_{xx}(\tau)] = \int_{-\infty}^{\infty} x(t)\left[\int_{-\infty}^{\infty} x(t')\exp[-j\omega(t'-t)]dt'\right]dt$$

$$
\begin{aligned}
&= \int_{-\infty}^{\infty} x(t) \left[\int_{-\infty}^{\infty} x(t') \exp[-j\omega t'] \exp[j\omega t] dt' \right] dt \\
&= \int_{-\infty}^{\infty} x(t) \exp[j\omega t] \left[\int_{-\infty}^{\infty} x(t') \exp[-j\omega t'] dt' \right] dt \\
&= \underbrace{\int_{-\infty}^{\infty} x(t) \exp[j\omega t] dt}_{X^*(\omega)} \underbrace{\int_{-\infty}^{\infty} x(t') \exp[-j\omega t'] dt'}_{X(\omega)} \\
&= X^*(\omega) X(\omega) \\
&= |X(\omega)|^2.
\end{aligned}
$$

Therefore,

$$FT[\phi_{xx}(\tau)] = |X(\omega)|^2,$$

that is, the Fourier transform of the autocorrelation function of a signal is the power spectral density of the signal.

4. n/a.

5. Given $y(t) = \alpha x(t - t_o) + \eta(t)$.

$$
\begin{aligned}
E[y(t)] &= E[\alpha x(t - t_o) + \eta(t)] \\
&= E[\alpha x(t - t_o)] + E[\eta(t)] \\
&= E[\alpha x(t - t_o)] \\
&= \alpha E[x(t - t_o)] \\
&= \alpha E[x(t)] \\
&= \alpha \mu_x.
\end{aligned}
$$

Because $x(t)$ is stationary, a change in the time origin is inconsequential; hence, $E[x(t - t_o)] = E[x(t)]$. Also, the mean of the noise is zero; hence, $E[\eta(t)] = 0$.

The ACF of $y(t)$ is obtained as follows:

$$
\begin{aligned}
E[y(t)y(t + \tau)] &= E[\{\alpha x(t - t_o) + \eta(t)\}\{\alpha x(t + \tau - t_o) + \eta(t + \tau)\}] \\
&= E[\alpha^2 x(t - t_o)x(t + \tau - t_o) + \alpha x(t - t_o)\eta(t + \tau) \\
&\quad + \alpha x(t + \tau - t_o)\eta(t) + \eta(t)\eta(t + \tau)] \\
&= E[\alpha^2 x(t - t_o)x(t + \tau - t_o)] + E[\alpha x(t - t_o)\eta(t + \tau)] \\
&\quad + E[\alpha x(t + \tau - t_o)\eta(t)] + E[\eta(t)\eta(t + \tau)].
\end{aligned}
$$

Because $x(t)$ is stationary, a change in the time origin is inconsequential; hence, $E[x(t - t_o)x(t + \tau - t_o)] = E[x(t)x(t + \tau)] = \phi_{xx}(\tau)$. Because $x(t)$ and $\eta(t)$ are statistically independent, their cross-correlation is zero; hence, $E[x(t)\eta(t+\tau)] = E[x(t + \tau)\eta(t)] = 0$. Thus, we have

$$E[y(t)y(t + \tau)] = \phi_{yy}(\tau) = \alpha^2 \phi_{xx}(\tau) + \phi_{\eta\eta}(\tau).$$

6. Given $x(t) = \sin(\omega_o t)$.

$$\begin{aligned}\phi_{xx}(\tau) &= \frac{1}{T}\int_0^T x(t)x(t+\tau)dt \\ &= \frac{1}{T}\int_0^T \sin(\omega_o t)\sin[\omega_o(t+\tau)]dt.\end{aligned}$$

Observe that, because the signal is periodic, we need to evaluate the integral over only one period; that is, from 0 to T.

We have the following trigonometric identities:

$$\cos(A+B) = \cos(A)\cos(B) - \sin(A)\sin(B).$$

$$\cos(A-B) = \cos(A)\cos(B) + \sin(A)\sin(B).$$

It follows that

$$\sin(A)\sin(B) = \frac{1}{2}[\cos(A-B) - \cos(A+B)].$$

Then, we have

$$\begin{aligned}\phi_{xx}(\tau) &= \frac{1}{2T}\int_0^T \{\cos[\omega_o t - \omega_o(t+\tau)] - \cos[\omega_o t + \omega_o(t+\tau)]\} \\ &= \frac{1}{2T}\int_0^T \{\cos(-\omega_o\tau) - \cos[\omega_o(2t+\tau)]\}dt \\ &= \frac{1}{2T}\left[\int_0^T \cos(-\omega_o\tau)dt - \int_0^T \cos[\omega_o(2t+\tau)]dt\right] \\ &= \frac{1}{2T}\left[\cos(-\omega_o\tau)\int_0^T dt - \int_0^T \cos[\omega_o(2t+\tau)]dt\right].\end{aligned}$$

The second integral above reduces to zero, because the area under a sinusoidal curve over a full period or an integral number of periods is zero. Observe also that $\cos(-\omega_o\tau)$ is independent of t. Then, we have

$$\begin{aligned}\phi_{xx}(\tau) &= \frac{1}{2T}[\cos(-\omega_o\tau)]T \\ &= \frac{1}{2}\cos(\omega_o\tau).\end{aligned}$$

Now, the PSD of the signal is given as

$$\begin{aligned}S_{xx}(\omega) &= FT[\phi_{xx}(\tau)] \\ &= \frac{1}{2}\int_0^T \cos(\omega_o\tau)\exp(-j\omega\tau)d\tau\end{aligned}$$

$$
\begin{aligned}
&= \frac{1}{4}\int_0^T [\exp(j\omega_o\tau) + \exp(-j\omega_o\tau)]\exp(-j\omega\tau)d\tau \\
&= \frac{1}{4}\int_0^T \exp[-j(\omega-\omega_o)\tau]d\tau + \frac{1}{4}\int_0^T \exp[-j(\omega+\omega_o)\tau]d\tau \\
&= \frac{2\pi}{4}\delta(\omega-\omega_o) + \frac{2\pi}{4}\delta(\omega+\omega_o).
\end{aligned}
$$

Therefore, the ACF of a sine wave is a cosine wave. The PSD of the sine wave has two impulses at $\omega = \pm\omega_o$.

7. The theta wave is being approximated as $\sin(2\pi\,5\,t)$. We saw in Problem 6 that the ACF of $\sin(\omega_o t)$ is $\phi(\tau) = \frac{1}{2}\cos(\omega_o\tau)$. Therefore, the ACF of the theta wave is $\phi(\tau) = \frac{1}{2}\cos(2\pi\,5\,\tau)$, which is shown in Figure 4.1. The frequency of the ACF is 5 Hz; therefore, the period is 0.2 s. The sampling frequency is $f_s = 100$ Hz, which corresponds to a sampling period of $T = 0.01$ s. Therefore, within an interval of 0.2 s, there are 20 samples, and within an interval of 0.5 s, there are 50 samples.

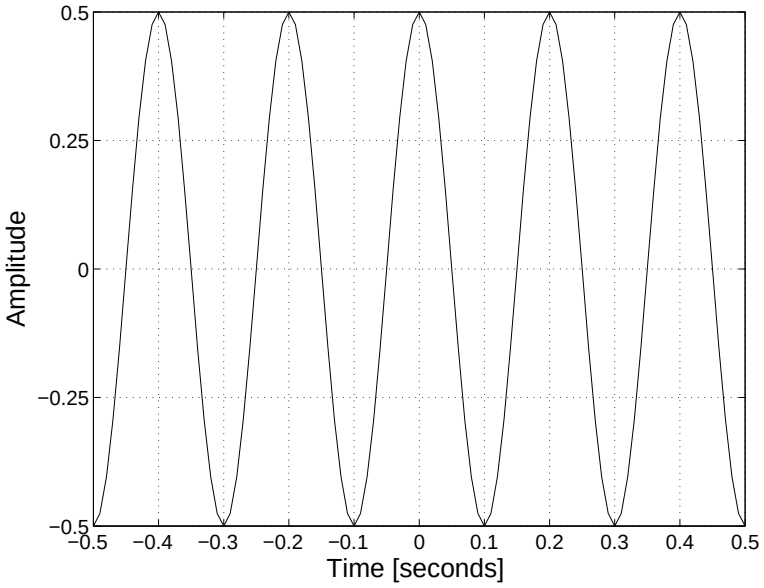

Figure 4.1: The ACF of a sine wave of frequency 5 Hz, shown for $\tau = \pm 0.5$ s. If the sampling frequency is 100 Hz, we have 10 samples for each portion of the plot corresponding to 0.1 s.

From Problem 6, we have the PSD of the signal given by

$$S(f) = \frac{1}{4}\delta(f-5) + \frac{1}{4}\delta(f+5), \tag{4.2}$$

where the frequency variable has been changed from ω to f, which has the effect

of removing the 2π factor. The PSD is shown in Figure 4.2.

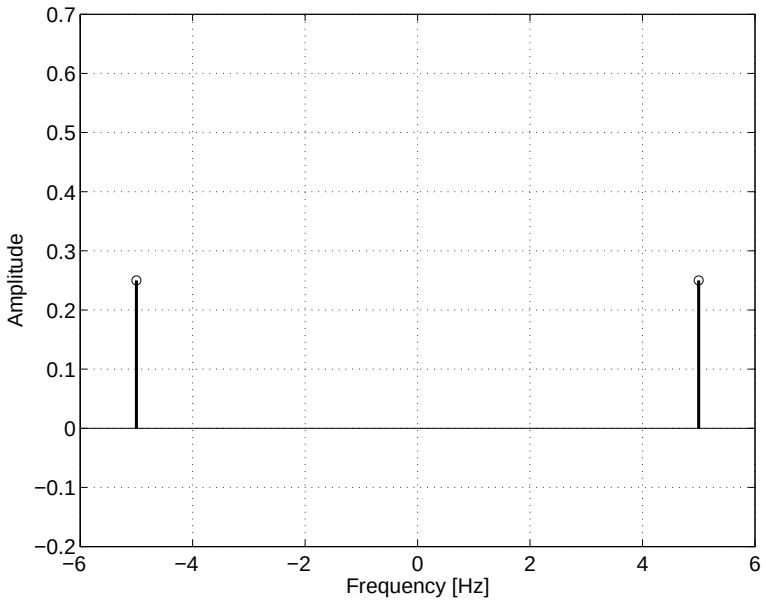

Figure 4.2: The PSD of a sine wave of frequency 5 Hz.

Because the signal is sampled at 100 Hz, the PSD is copied at ± 100, ± 200, $\ldots$, $\pm n100$ Hz; that is, there will be additional impulses at ± 95, ± 105, ± 195, $\ldots$ Hz.

8. The template given is $x(n) = \{0, 5, 5, 5, 0\}$. The signal given may be written in terms of the template as

$$y(n) = 2x(n-3) + x(n-11) - \frac{3}{5}x(n-19).$$

Based upon Problem 5, we have the cross-correlation between $x(t)$ and $y_1(t) = \alpha x(t - t_o)$ as

$$\begin{aligned} \theta_{xy_1}(\tau) &= E[y_1(t+\tau)x(t)] \\ &= E[\alpha x(t+\tau-t_o)x(t)] \\ &= \alpha\phi_{xx}(\tau - t_o). \end{aligned}$$

The given signal has three scaled and shifted copies of the template. Therefore,

$$\theta_{xy}(\tau) = 2\phi_{xx}(\tau-3) + \phi_{xx}(\tau-11) - \frac{3}{5}\phi_{xx}(\tau-19).$$

The ACF $\phi_{xx}(\tau)$ of $x(t)$ is obtained as follows:

$x(t)$	0	5	5	5	0		
$x(t-0)$	0	5	5	5	0		$\rightarrow \phi_{xx}(0) = 75$
$x(t-1)$		0	5	5	5	0	$\rightarrow \phi_{xx}(-1) = 50$
$x(t-2)$			0	5	5	...	$\rightarrow \phi_{xx}(-2) = 25$
$x(t-3)$				0	5	...	$\rightarrow \phi_{xx}(-3) = 0$

From the symmetry property of the ACF, we also have $\phi_{xx}(1) = \phi_{xx}(-1) = 50$, $\phi_{xx}(2) = \phi_{xx}(-2) = 25$. Observe that $\phi_{xx}(\tau) = 0$ for $|\tau| > 2$ for the template given.

The procedure for numerical computation of the cross-correlation function between $y(n)$ and $x(n)$ is shown in Table 4.1.

The signals $x(n)$ and $y(n)$ are plotted in Figure 4.3. The signal $y(n)$ and the result of template matching (cross-correlation function) are plotted in Figure 4.4. The peaks in the result occur at the beginning of each copy of the template in the signal $y(n)$ because of the manner in which the template is configured. If matched filtering is performed with a causal version of the reversed version of the template, the results will be shifted by the duration of the template; this result is shown in Figure 4.5.

9. n/a.

10. n/a.

0	1	2	3	4	5	6	7	8	9	10	11	12	13	14	15	16	17	18	19	20	21	22	23
0	50	100	150	100	50	0	0	0	25	50	75	50	25	0	0	0	-15	-30	-45	-30	-15	0	0
0	0	0	0	10	10	10	0	0	0	0	0	5	5	5	0	0	0	0	0	-3	-3	-3	0
0	5	5	5	0																			
	0	5	5	5	0																		
		0	5	5	5	0																	
			0	5	5	5	0																
				0	5	5	5	0															
					0	5	5	5	0														
						0	5	5	5	0													
							0	5	5	5	0												
								0	5	5	5	0											
									0	5	5	5	0										
										0	5	5	5	0									
											⋱	⋱	⋱	⋱	⋱								

Table 4.1: Computation of the cross-correlation function for Problem 4.8. The top three rows represent the delay τ, the cross-correlation function $\theta_{xy}(\tau)$, and the signal $y(n)$. The subsequent rows represent $x(n-\tau)$ for various values of τ.

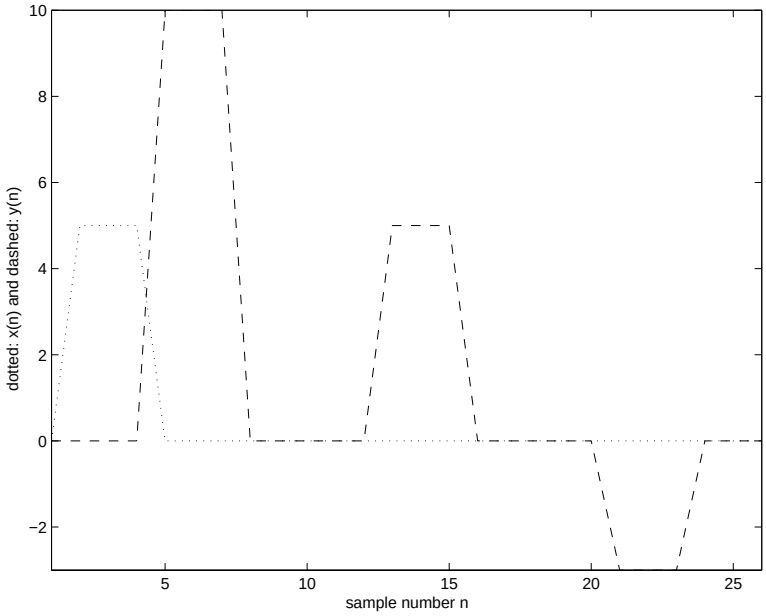

Figure 4.3: The template and the given signal in Problem 4.8.

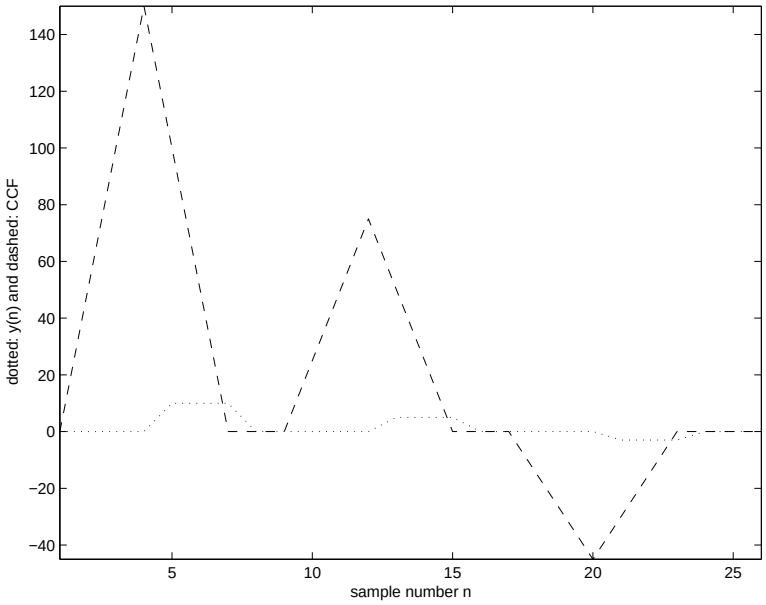

Figure 4.4: The cross-correlation function and the given signal in Problem 4.8.

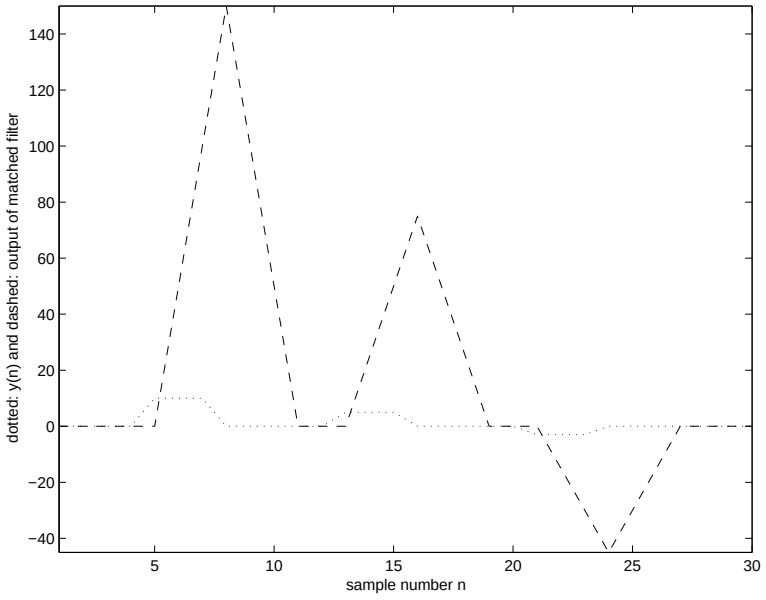

Figure 4.5: Problem 4.8: The given signal $y(n)$ and the result of matched filtering.

Chapter 5

Solutions to Selected Problems

1. The form factor FF is based upon the variance of the given signal $x(t)$ and the variance of its first and second derivatives $x'(t)$ and $x''(t)$, respectively. Using σ to denote the standard deviation, which is the square root of the variance, we have

$$FF = \frac{\sigma_{x''}/\sigma_{x'}}{\sigma_{x'}/\sigma_x}.$$

Given

$$x(t) = \sin(\omega t),$$

we have

$$x'(t) = \omega \cos(\omega t),$$

and

$$x''(t) = -\omega^2 \sin(\omega t).$$

Because the mean value of a sine or cosine function (computed over one period) is zero, the variance is given by the mean-squared value; that is,

$$E[(x - \mu_x)^2] = E[x^2].$$

Because we are given a function of time that is periodic, we can compute the time-average mean-squared value by integrating over one period T as follows:

$$\begin{aligned}
\sigma_x^2 &= \frac{1}{T}\int_0^T \sin^2(\omega t)\, dt \\
&= \frac{1}{T}\int_0^T \frac{1}{2}[1 - \cos(2\omega t)]\, dt \\
&= \frac{1}{2T}\int_0^T dt - \frac{1}{2T}\int_0^T \cos(2\omega t)\, dt
\end{aligned}$$

$$= \frac{1}{2T} T - 0$$
$$= \frac{1}{2}.$$

Observe that the integral of a sinsoidal function over an integral multiple of its period is zero.

In a similar manner, it can be shown that the mean-squared value of a cosine wave is also $\frac{1}{2}$.

It follows that

$$\sigma_{x'}^2 = \frac{\omega^2}{2},$$

and

$$\sigma_{x''}^2 = \frac{\omega^4}{2}.$$

Then, we have

$$FF = 1.$$

2. Similar question on 1999 Final Exam. Will work out in class/ tutorial.

3. Template matching is performed by computing the cross-correlation between the given template and the signal, as follows:

$y(n)$	0	0	2	2	3	-3	2	0	0	
$x(n+0)$	1	-1								$\theta_{xy}(0) = 0$
$x(n+1)$		1	-1							$\theta_{xy}(1) = -2$
$x(n+2)$			1	-1						$\theta_{xy}(2) = 0$
$x(n+3)$				1	-1					$\theta_{xy}(3) = -1$
$x(n+4)$					1	-1				$\theta_{xy}(4) = 6$
$\ddots$						$\ddots$	$\ddots$			$\ddots$

Continuing the procedure shown above, we get the output of template matching as

$\{0, -2, 0, -1, 6, -5, 2, 0\}$.

The output is expected to show peaks at the locations of patterns that match the template. In the given signal, the pattern that matches the template is $\{3, -3\}$, which is given as three times the template. The result of the template-matching procedure, plotted in Figure 5.1, has its maximum (value = 6) at the location of the pattern $\{3, -3\}$ in the input signal. Note, however, that the pattern $\{-3, 2\}$ in the signal also matches the template in a reverse sense, to some extent. The output value of -5 at the location of this pattern is the second largest value of the output (in magnitude).

4. n/a.

5. n/a.

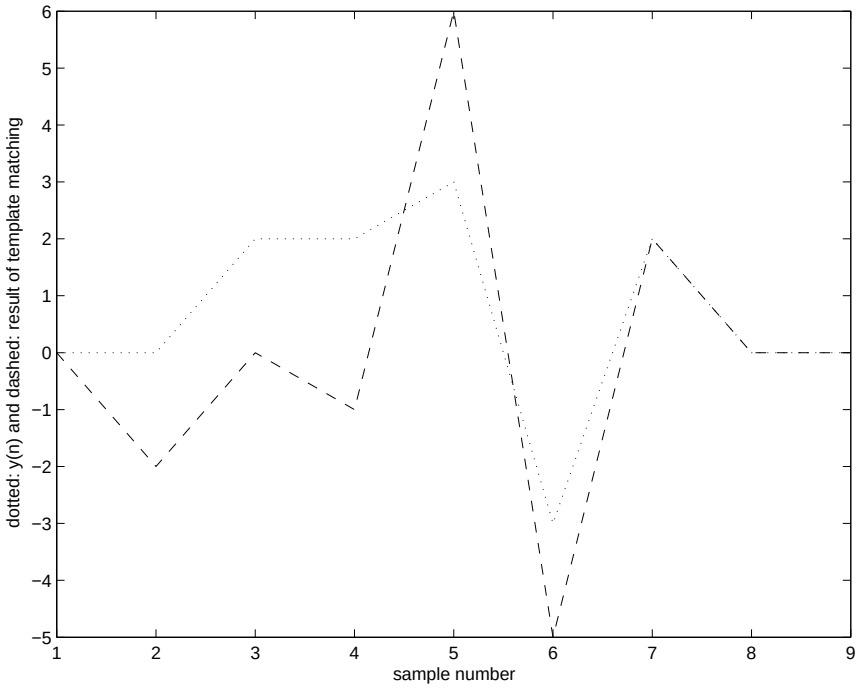

Figure 5.1: Problem 5.3: Signal given and the result of template matching.

6. n/a.

7. Question on 1999 Final Exam. Will work out in class/ tutorial.

8. Question on 1999 Final Exam. Will work out in class/ tutorial.

9. n/a.

Chapter 6

Solutions to Selected Problems

1. *Correction:* For the sake of circular or periodic convolution, the two signals need to be of the same duration or period. For this reason, change the impulse response from $\{3, 1, -1\}$ to $\{3, 1, -1, 1\}$.

(a) The output of the filter is given by the *linear* convolution of the input signal with the impulse response.

Convolving $\{3, 1, -1, 1\}$ with $\{4, 4, 2, 1\}$ in a linear manner, we get the output as

$\{12, 16, 6, 5, 3, 1, 1\}$.

Observe that the input signal and the impulse response each have four samples; the number of samples in the result of linear convolution is $4 + 4 - 1 = 7$.

(b) *Linear* convolution.

(c) The result of *circular* or *periodic* convolution will have the same period or number of samples as the two signals being convolved. In this example, the output will have four samples.

Considering a window over one period of the signals, circular shifting for periodic convolution is performed as follows:

Impulse response :	3	1	−1	1	
Input signal :	4	4	2	1	*Output*
Reversed; *Shift* 0 :	4	1	2	4	15
Shift 1 :	4	4	1	2	17
Shift 2 :	2	4	4	1	7
Shift 3 :	1	2	4	4	5

(6.1)

Observe that, in reversing a periodic signal (with period of $N = 4$ samples in the present example), we have the following results:

$x(-1) = x(N-1) = x(4-1) = x(3) = 1$
$x(-2) = x(N-2) = x(4-2) = x(2) = 2$
$x(-3) = x(N-3) = x(4-3) = x(1) = 4$
$x(0)$ remains unchanged.
The indexing of the samples within a period is: 0, 1, 2, 3.

(d) If we take the DFTs of two signals using a DFT array of the same size as the signals, multiply the DFT arrays on a point-by-point by basis, and take the inverse DFT of the resulting array, we get the result of *circular* or *periodic* convolution. In this case, note that all arrays are of the same duration or number of samples.

The result of the DFT-based procedure described above may be made equal to that of linear convolution by padding zeros to both signals such that their lengths are at least equal to the number of samples expected in the result of linear convolution. If the signals to be convolved have L_1 and L_2 samples, the result of linear convolution will have $L_r = L_1 + L_2 - 1$ samples. By taking the DFTs of the zero-padded signals with an array size of at least L_r samples, multiplying the DFT arrays on a point-by-point by basis, and taking the inverse DFT of the resulting array, the result of the inherent periodic convolution can be made equivalent to the result of linear convolution.

2. The Fourier transform $X(\omega)$ of a discrete-time signal $x(n)$ is given by

$$FT[x(n)] = X(\omega) = \sum_{n=0}^{N-1} x(n) \exp(-j\omega n). \tag{6.2}$$

Consider the signal $x^*(-n)$, which is the conjugated and reversed version of $x(n)$. Because $x(n)$ exists for $n = 0, 1, 2, \ldots, N-1$, $x^*(-n)$ will exist for $n = 0, -1, -2, \ldots, -(N-1)$.

Now, consider the Fourier transform $X_1(\omega)$ of $x^*(-n)$, which is given as

$$X_1(\omega) = FT[x^*(-n)] = \sum_{n=-(N-1)}^{0} x^*(-n) \exp[-j\omega n].$$

Now, let us change the index variable $-n$ to m. Then, we have

$$\begin{aligned} X_1(\omega) &= \sum_{m=0}^{N-1} x^*(m) \exp[+j\omega m] \\ &= \sum_{m=0}^{N-1} x^*(m) \{\exp[-j\omega m]\}^* \\ &= X^*(\omega), \end{aligned}$$

with the last step obtained in comparison with the definition in Equation 6.2.

Now,

$$x_e(n) = \frac{1}{2}[x(n) + x^*(-n)].$$

Therefore,

$$\begin{aligned} FT[x_e(n)] &= \frac{1}{2}\{FT[x(n)] + FT[x^*(-n)]\} \\ &= \frac{1}{2}\{X(\omega) + X^*(\omega)\} \\ &= Re[X(\omega)]. \end{aligned}$$

It follows that the Fourier transform of an even-symmetric function (signal) is a real function; that is, its imaginary part is zero. This implies that the phase spectrum of the signal is zero for all frequencies, and that the signal is composed of cosine functions only.

Similarly, we have

$$\begin{aligned} FT[x_o(n)] &= \frac{1}{2}\{FT[x(n)] - FT[x^*(-n)]\} \\ &= \frac{1}{2}\{X(\omega) - X^*(\omega)\} \\ &= j\, Im[X(\omega)]. \end{aligned}$$

It follows that the Fourier transform of an odd-symmetric function (signal) is an imaginary function; that is, its real part is zero. This implies that the signal is composed of sine functions only.

Note that the projection of an even-symmetric function onto an odd-symmetric function is zero.

3. See Problems 5 and 3 in Chapter 4.

4. Question on 1999 Final Exam. Will work out in class/ tutorial. See also Problems 6 and 7 in Chapter 4.

5. The DFT $X_1(k)$ of $x_1(n)$ is given, by definition, as

$$DFT[x_1(n)] = X_1(k) = \sum_{n=0}^{N-1} x_1(n) \exp\left(-j\frac{2\pi}{N}nk\right). \tag{6.3}$$

Given $x_1(n)$ is real, it follows that

$$\begin{aligned} X_1^*(k) &= \sum_{n=0}^{N-1} x_1(n) \exp\left(+j\frac{2\pi}{N}nk\right) \\ &= X_1(-k); \end{aligned} \tag{6.4}$$

that is, the DFT of a real signal possesses conjugate-symmetry.

Now, we have two signals $x_1(n)$ and $x_2(n)$ combined as

$$y(n) = x_1(n) + j\, x_2(n).$$

Due to the linearity of the Fourier transform, we have the DFT $Y(k)$ of $y(n)$ as

$$Y(k) = X_1(k) + j\,X_2(k). \tag{6.5}$$

Now, $X_1(k)$ and $X_2(k)$ are complex, and may be expressed in terms of their real and imaginary parts as

$$X_1(k) = Re[X_1(k)] + j\,Im[X_1(k)]$$

and

$$X_2(k) = Re[X_2(k)] + j\,Im[X_2(k)].$$

Similarly, $Y(k)$ is also complex, and may be expressed in terms of the real and imaginary parts of $X_1(k)$ and $X_2(k)$ as

$$\begin{aligned} Y(k) &= Re[X_1(k)] + j\,Im[X_1(k)] + j\,\{Re[X_2(k)] + j\,Im[X_2(k)]\} \\ &= \{Re[X_1(k)] - Im[X_2(k)]\} + j\,\{Im[X_1(k)] + Re[X_2(k)]\}. \end{aligned}$$

It follows that

$$\begin{aligned} Y^*(k) &= \{Re[X_1(k)] - Im[X_2(k)]\} - j\,\{Im[X_1(k)] + Re[X_2(k)]\} \\ &= \{Re[X_1(k)] - j\,Im[X_1(k)]\} - j\,\{Re[X_2(k)] - j\,Im[X_2(k)]\} \\ &= X_1^*(k) - j\,X_2^*(k). \end{aligned} \tag{6.6}$$

We also have

$$\begin{aligned} Y^*(-k) &= X_1^*(-k) - j\,X_2^*(-k) \\ &= X_1(k) - j\,X_2(k), \end{aligned} \tag{6.7}$$

where the last step follows from the conjugate-symmtery property of the DFT of a real signal, stated in Equation 6.4. Combining Equations 6.5 and 6.7, we get

$$Y(k) + Y^*(-k) = 2X_1(k),$$

leading to

$$X_1(k) = \frac{1}{2}[Y(k) + Y^*(-k)] = Y_e(k);$$

that is, the DFT of $x_1(n)$ is given by the even part of the DFT of the combined signal $y(n)$.

Similarly, we have

$$Y(k) - Y^*(-k) = 2j\,X_2(k),$$

leading to

$$X_2(k) = \frac{1}{2j}[Y(k) - Y^*(-k)] = -j\,Y_o(k);$$

that is, the DFT of $x_1(n)$ is given by the odd part of the DFT of the combined signal $y(n)$, with the scale factor of $-j$.

The net result is that the DFTs of two real signals may be computed using only one DFT procedure. Note that a general DFT procedure is designed to accept a complex input and generate a complex output. The properties derived above indicate that computational savings may be achieved by computing the DFT of the combined signal, which may then be used to recover the DFTs of the two individual signals.

6. n/a.

7. n/a.

8. n/a.